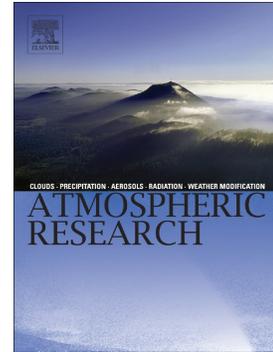# Accepted Manuscript

Contribution to column-integrated aerosol typing based on Sun-photometry using different criteria

I. Foyo-Moreno, I. Alados, J.L. Guerrero-Rascado, H. Lyamani, D. Pérez-Ramírez, F.J. Olmo, L. Alados-Arboledas

Please cite this article as: I. Foyo-Moreno, I. Alados, J.L. Guerrero-Rascado, et al., Contribution to column-integrated aerosol typing based on Sun-photometry using different criteria, Atmospheric Research, https://doi.org/10.1016/j.atmosres.2019.03.007

Contribution to column-integrated aerosol typing based on Sun-photometry using different criteria

I. Foyo-Moreno (1,2), I. Alados (2,3), J.L. Guerrero-Rascado (1,2), H. Lyamani (2), D. Pérez-Ramírez, (1,2), F.J. Olmo (1,2) and L. Alados-Arboledas (1,2).

(1) Applied Physics Department, University of Granada, Fuentenueva s/n, 18071, Granada, Spain.

(2) Andalusian Institute for Earth System Research (IISTA-CEAMA), Avda. del Mediterráneo s/n, 18006, Granada, Spain.

(3) Applied Physics II Department, University of Málaga, Campus de Teatinos s/n, 29071, Málaga, Spain.

Corresponding author: ifoyo@ugr.es

Abstract

This study analyses the aerosol optical and microphysical properties obtained by the Aerosol Robotic Network (AERONET) in seven different sites operating in the Iberian Peninsula during three coincident years (2010-2012) with the objective of studying different aerosol typing approaches. This area is of interest due to its location between the Sahara desert (the largest source of natural aerosols in the world) and mainland Europe (a relevant source of anthropogenic aerosols). In particular, we study the aerosol optical depth (AOD), Angström parameter ($\alpha_{440-870}$) and fine mode fraction (FMF), which are estimated from direct sun irradiance measurements. Additionally, the single scattering albedo (ω_o) and aerosol particle size distribution (PSD), which are computed using additional sky radiances measurements under cloudless skies, are used in our analyses. The analyses show aerosol seasonal patterns in the AOD with maximum values in summer/spring and minimum values in winter/autumn for all the analysed stations. For $\alpha_{440-870}$, there are differences from site to site, with maximum values in winter and minimum values in summer for the southern locations, while there is not a remarkable pattern for the eastern locations close to the Mediterranean coast. The frequent and intense Saharan dust outbreaks over the southern Iberian Peninsula and the intense anthropogenic activity in the eastern urban locations are behind these seasonal patterns in the AOD and $\alpha_{440-870}$. In this work, two of the most employed classification schemes of aerosol type in the literature are used: one is based on the AOD and $\alpha_{440-870}$, the other one is based on ω_o at 440 nm and the FMF and a new classification scheme based on ω_o at 440 nm and FMF is proposed. The results revealed that the new classification method is more appropriate for distinguishing the aerosol types that affect the Iberian Peninsula. The relationship derived here between $\Delta\omega_o = \omega_o(440) - \omega_o(1020)$ and the FMF is demonstrated to be useful for aerosol type classification when no

measurements of the sky radiances, and consequently of $\omega_o(440)$, are available. Alternatively, the relationship between the ratio $\Delta\omega_o/\omega_o(440)$ and the FMF can be used because $(\Delta\omega_o/\omega_o)$ provides information about both the spectral ω_o and the absolute values.

1. Introduction

Knowledge of atmospheric aerosols is especially important because they contribute to global and regional climate variability (Boucher et al., 2013). Aerosols are known to influence the Earth's energy budget and climate directly, by scattering and absorbing solar radiation (Queface et al., 2011), and indirectly, by acting as cloud condensation and ice nuclei, thereby modifying cloud properties and the cloud lifetime and perturbing the global water cycle, among others (Boucher et al., 2013). Furthermore, aerosol particles have an appreciable influence on air quality (Lyamani et al., 2012), visibility (Horvath, 1995), human health (Dockery and Pope, 1996; Kampa and Castana, 2008), and atmospheric chemical processes (Schwartz, 1994). Understanding and quantifying the influence of atmospheric aerosols on the Earth's energy balance and on the environment requires accurate knowledge of their physical and optical properties, especially their sizes and absorption properties, as well as detailed information on the aerosol type (Boucher et al, 2013).

During the past few years, a large effort has been made to characterize the effects of atmospheric aerosols on the Earth's radiative balance and climate. Consequently, the uncertainty in aerosol radiative forcing (that is, the perturbation to Earth's energy budget) has been substantially reduced. The level of confidence of atmospheric aerosols effects has increased from medium to high for the direct effect and from low to medium for the indirect effect (Boucher et al., 2013).

Despite substantial progress in the assessment of aerosol effects in the last few years, several important issues remain, and significant efforts are required to address

them. The uncertainty in the total aerosol radiative forcing estimate is still substantial compared to the uncertainties associated with the greenhouse gases effect). Additionally, the uncertainties in the individual radiative forcing of several aerosol components, such as black carbon (BC) and desert dust, are still large. Furthermore, the uncertainties in the aerosol radiative effect estimates are larger on regional scales than on the global scale (Boucher et al., 2013).

These aerosol effect uncertainties are mostly due to the high spatial and temporal variations of the physical, optical and chemical properties of aerosols, and the limited information on the absorption properties of aerosols (key variables for estimating aerosol radiative effects) as well as the aerosol types (Boucher et al., 2013). Thus, there is still a real need for characterizing the atmospheric aerosol load and aerosol types, as well as their optical and physical properties, especially their size and absorption properties, at the regional scale at sufficiently high temporal and spatial resolutions to better understand aerosol effects and reduce aerosol radiative effect uncertainties. This characterization is even more needed in the case of highly polluted and climatic sensitive regions, such as the Mediterranean basin (Boucher et al., 2013).

Due to its geographical position, the Western Mediterranean basin is characterized by the presence of a large variety of aerosol types, including anthropogenic aerosols transported from European and North African urban areas, desert dust originating from arid areas of North African, maritime aerosols from the Mediterranean Sea and Atlantic Ocean (e.g., Valenzuela et al., 2014, Mateos et al., 2014), biomass burning aerosols from forest fires, and anthropogenic particles emitted from the intense ship traffic in the Mediterranean Sea (e.g., Lyamani et al., 2015). For this reason, the aerosol load and aerosol radiative forcing over the Mediterranean basin are among the highest in the world, especially in summer (e.g. Markowicz et al., 2002;

Papadimas et al., 2012). However, the estimated aerosol radiative forcing in the Mediterranean area is largely uncertain (Mallet et al., 2013).

Although several studies on the characterization of columnar aerosol properties have been conducted over the Western Mediterranean, especially over the Iberian Peninsula, the majority of these studies focused their analysis at only one site (e.g., Obregón et al., 2015, Bennouna et al., 2011) and many of them were of relatively short duration (e.g., Elias et al., 2006; Lyamani et al., 2006a, 2006b; Prats et al., 2008). The use of AERONET measurements has served as a long-term analysis of the optical and microphysical properties of aerosols in the Iberian Peninsula and the most robust statistical analysis was presented by Mateos et al. (2015), who analysed more than 10 years of data obtained at all AERONET Iberian Peninsula stations. This study complements the first studies of a decade ago performed individually for certain regions of the Iberian Peninsula (e.g., Alados-Arboledas et al., (2003) for the southeast region, Toledano et al. (2007) for the southwest region, Estellés et al. (2007) for the Mediterranean region, Bennouna et al. (2013) for the north-central region and Silva et al. (2002) for the eastern region). The continuation of AERONET measurements and the deployment of new stations in the Iberian Peninsula will serve for more robust climatological studies when more years of data are available. Nevertheless, the complexity of aerosol types in the Iberian Peninsula makes the region ideal for studying aerosol-typing schemes.

The main objective of this work is to study different aerosol typing approaches using the large variability of aerosol properties at key sites of the Iberian Peninsula, covering different aerosol types representative of marine, rural and urban aerosols. The spatial and temporal variability of columnar aerosol's optical and microphysical properties are analysed to better understand aerosol typing. The data used in this work

are from the Aerosol Robotic Network (AERONET) for the period of 2010-2012 at seven representative sites in the Iberian Peninsula. We focus on the aerosol optical depth (AOD), the Angstrom parameter ($\alpha_{440-870}$) and the Fine Mode Fraction (FMF), which is retrieved from direct Sun measurements. Additionally, the aerosol particle size distribution (PSD) and single scattering albedo (ω_0) from the AERONET inversion products are analysed (Dubovik et al., 2000; 2006).

The paper is structured as follows: Section 2 describes the different AERONET sites selected in our analyses and the AERONET measurements and datasets. Section 3 analyses and discusses the scientific results, and conclusions are given in Section 4.

2. Measurement sites and dataset

Figure 1 shows the locations of the different AERONET stations used in this work (Barcelona, Burjassot, Cáceres, Évora, Granada, Huelva and Málaga). These sites were selected with the objective of covering different environmental conditions of the Iberian Peninsula and different background aerosols, including urban, coastal and rural sites. Additionally, the sites were selected for continuous AERONET measurements for the study period (2010-2012). The selected sites and the study period used provide almost all aerosol loads and types known in the atmosphere, including fine and coarse mode predominance of particles, absorbing and non-absorbing particles and mixtures among all these aerosol types. The details of each station can be found in the bibliography as they are very well known AERONET sites, but here we provide a short overview.

Barcelona is one of the most densely populated cities in Spain, with more than 3 million inhabitants. Barcelona is located in the North-East of Spain on the

Mediterranean side and is a highly industrialised agglomerated city. Anthropogenic emissions from industrial activities, road and shipping traffic are the main sources of pollution in this city (Pérez et al., 2016). The small city of Burjassot (35,000 inhabitants) is located 5 km northwest from the centre of Valencia (approximately 1.5 million) and 10 km west from the Mediterranean coast. Light industry is found in this area and varied intensive agriculture is also practiced in the region. Cáceres is a unique AERONET station in the vast region of Extremadura, Spain and is located outside the city (approximately 90 000 inhabitants) and almost 250 km eastward from the Portuguese coast. Different aerosol types, namely industrial/urban as well as Saharan mineral dust and forest fire aerosol particles influence the area (Obregón et al., 2009). This station is considered a good representative case of the Western Spain region (Obregón et al., 2015). Évora (Portugal) is a small city (approximately 55 000 inhabitants) located in the south-western part of the Iberian Peninsula. Located in a rural area, it is remote from sources of industrial pollution, and 100 km away from the Atlantic coast. Local pollution is only due to private cars, as no large industries work in the area. The nearest large urban and industrialized area is Lisbon (approximately 1 million inhabitants) at 100 km away from Évora. Granada, situated in the south-eastern region of Spain, is a non-industrialised, medium-size city with a population of 240 000 inhabitants, where road traffic and winter domestic heating represent the major anthropogenic source of pollution (Titos et al., 2017; Patrón et al., 2017). The Huelva AERONET station is located in a rural area in south-western Spain (Huelva region), in the Atlantic coastal area of the Cadiz Gulf. This station is surrounded by a pine tree forest and Doñana National Park, one of the largest and most unique natural reservoir areas in Europe. Local aerosols are mainly maritime; however, the site can also be affected by industrial pollutants emitted 15–30 km away from the station by the

industrial belt of Palos–Huelva (López et al., 2015). Málaga (approximately 600 000 inhabitants) is a major coastal city in south-eastern Spain on the Mediterranean coast and is located approximately 150 km southeast of Granada, and the main sources of pollution in this city are road and shipping traffic.

The standard instrument used in AERONET is the Cimel 318 radiometer, which performs direct Sun measurements at selected wavelengths in the spectral range of 340-1020 nm. Furthermore, the instrument also measures sky radiance in the solar almucantar and the principal plane configurations at 440, 670, 870 and 1020 nm. The direct Sun observations are used to derive the spectral aerosol optical depth (AOD) and the Angstrom exponent, $\alpha_{440-870}$ (computed using the wavelengths between 440 and 870 nm). A value of $\alpha_{440-870} > 1$ indicates the dominance of fine particles mainly from the combustion-related anthropogenic sources, whereas $\alpha_{440-870} < 1$ indicates the dominance of coarse particles, such as desert mineral dust and sea salt particles (Eck et al., 1999). Additionally, we used AERONET aerosol optical depths associated with fine (AOD_{fine}) and coarse (AOD_{coarse}) mode particles, and the contribution of the fine mode to AOD at 500 nm, known as fine mode fraction (FMF), provided by the spectral deconvolution algorithm developed by O'Neill et al. (2003). The sky radiances together with the AOD are employed to retrieve a set of aerosol optical and microphysical properties via inversion methods (Dubovik and King, 2000; Dubovik et al., 2006). These include particle size distribution (PSD) and single scattering albedo (ω_o), among others.

More details on the AERONET measurement protocol, calibration techniques, methodology, data processing and quality can be found in the literature (Holben et al., 1998; Eck et al., 1999). In this study we use AERONET Level 2.0 data from version 2, whose data quality is guaranteed (Smirnov et al., 2000). AERONET data version 2 are highly used in the scientific community, although recently AERONET data version 3

has been established, which is more reliable in terms of cloud screening and in detecting instrumental anomalies (Giles et al., 2018). However, no appreciable difference between versions 2 and 3, at least in terms of AOD, was observed (Giles et al., 2018). For other aerosol parameters, the differences between versions 2 and 3 are not studied yet. Therefore, although version 3 may provide more reliable data for statistical studies and for the study of special events, the use of this version is not critical for our purposes of studying aerosol typing.

From the AERONET version 2 data the uncertainty in the AOD is of $\pm$ 0.01 for wavelengths $\geq$ 440 nm and of $\pm$ 0.02 for shorter wavelengths (Holben et al., 1998). he estimated uncertainty for the FMF is approximately 10% (O'Neill et al., 2003) and the error for $\alpha_{440-870}$ depends on the AOD values, with the error being higher for a low AOD. Wagner and Silva (2008) demonstrated that $\alpha_{440-870}$ will be systematically over- or underestimated depending on whether the relative error in AOD at shorter wavelength is larger or smaller compared with the relative error at longer wavelength, respectively. AERONET retrievals impose limitations in the scattering angle and aerosol load, with uncertainties in ω_0 being $\pm$ 0.03 when AOD(440) is > 0.40 and higher (0.05-0.07) when AOD(440) is < 0.20 (Dubovik et al., 2000).

3. Results and discussion

3.1. Temporal variation of aerosol properties

3.1.1. Spectral aerosol optical depth, Ångström exponent and fine mode fraction

Figure 2 shows the AOD(440) and $\alpha_{440-870}$ monthly mean values for each selected AERONET site during the study period (2010-2012). Some sites present gaps in the data set due to the maintenance of the stations and/or meteorological conditions not appropriate for AERONET measurements. The highest value of AOD(440) was

obtained at Barcelona in June 2012 (0.37 ± 0.20), while the lowest value was at Cáceres in November 2010 (0.03 ± 0.01). All the stations present an evident AOD annual pattern with a maximum in summer and minimum in winter. Actually, the larger frequency of the Saharan dust arrivals in summer could explain this increase during these months. In spite of the south-to-north gradient in dust intrusions, Saharan mineral dust particles seem to significantly contribute to the aerosol load over the entire Iberian Peninsula. However, the fact that larger AODs are found in Barcelona and Burjassot (urban areas) suggests a mixture of dust with local anthropogenic sources, which could be corroborated later with an analysis of the rest of the variables analysed in this work.

The seasonal pattern of $\alpha_{440-870}$ presents a minimum in summer and a maximum in winter for the southern stations (Granada, Huelva and Málaga). These places registered $\alpha_{440-870} < 0.6$ in summer, which indicates a clear predominance of dust particles in this season (Dubovik et al., 2002). Actually, Granada presents the lowest $\alpha_{440-870}$ value of the dataset in August 2012 (0.29 ± 0.10). This region is frequently affected by Saharan dust transport in summer, which justifies the presence of coarse particles (e.g., Pérez-Ramírez et al., 2016). Cáceres and Évora also present the same $\alpha_{440-870}$ seasonal patterns but they are considerably less pronounced than at southern stations. For the stations at the Eastern Iberian Peninsula (Barcelona and Burjassot), the seasonal pattern in $\alpha_{440-870}$ is not remarkable. The few anthropogenic emissions in Granada during summer (Lyamani et al., 2010) and the fact that Cáceres is almost considered to be a rural station (Obregón et al., 2015) suggests differences between the dust particles at each station, indicating the presence of larger particles in the southern locations. This difference in particle predominance can be explained by the deposition of the coarsest dust particles during their transport. The large $\alpha_{440-870}$ for Barcelona and Burjassot during summer support this south-to-north gradient in aerosol types.

Figure 3 shows the temporal evolution of the monthly means for the FMF and reveals interesting results. Coastal areas, such as Málaga, Barcelona and Burjassot do not present remarkable seasonal patterns, with just slightly larger values in winter. With the previous results of a large contribution of anthropogenic activities to these urban places, the FMF of ~ 0.80 for Barcelona and Burjassot and of ~ 0.5 for Málaga suggest a constant contribution of coarse particles. Because these places are close to the seashore, the influence of marine particles is not negligible. However, the more frequent arrivals of Saharan dust to the southern locations can explain the lower values of the FMF in Málaga. Huelva is also a coastal area that presents the lowest FMF, which can be explained by the large influence of marine particles. Other remote areas such as Cáceres and Évora also experienced a pattern similar to that observed in Huelva, but with generally larger FMF values, which is explained by the lack of influence of marine particles. Finally, Granada presents a unique seasonal pattern characterized by large values in winter of ~ 0.8 and low values in summer of ~ 0.4. This pattern is explained by the characteristics of the site: winters are characterized by a strong contribution of anthropogenic activity with a large contribution of fine particles. During summer, due to the reduced anthropogenic activity, the dryness of the terrain and the more frequent arrival of Saharan dust particles, the contribution of coarse particles is larger (Pérez-Ramírez et al., 2012).

Table 1 summarizes the statistical analysis using daily averages for AOD(440), $\alpha_{440-870}$ and FMF for all sites. Barcelona, Burjassot and Málaga present the highest mean value for the AOD(440) (0.19 ± 0.12 at Barcelona). Évora and Cáceres present the lowest mean values, 0.13 ± 0.10 and 0.14 ± 0.09, respectively. The lowest mean $\alpha_{440-870}$ values are found at Málaga and Huelva (0.93 ± 0.35, 0.93 ± 0.41, respectively) and the highest at Barcelona (1.31 ± 0.32). For the FMF, all locations have mean values above

0.50, suggesting a large contribution of fine particles to the total aerosol optical depth at 500 nm. The highest value of FMF is found at Cáceres (0.72 ± 0.17) and three localities (Málaga, Granada and Huelva) have the lowest mean values (close to 0.55), with a value of 0.53 ± 0.16 at Málaga. These FMF lowest values are explained by the proximity of these sites to the African continent, meaning this Mediterranean region more affected by the Saharan dust intrusions. Northern locations have the largest FMF values (~ 0.70), which are explained by the most intense anthropogenic activity and by less frequency and intensity of Saharan dust arrivals to these sites in comparison to southern locations. These results are in accordance to Mallet et al. (2013), who found a correlation between $\alpha_{440\text{-}870}$ and the station's latitude, with lower $\alpha_{440\text{-}870}$ values at Southern stations, where the influence of the desert dust is more significant.

To analyse the seasonal variations of the aerosol's optical properties at the studied sites, all data have been grouped into four seasons: winter (January-March), spring (April-June), summer (July-September) and autumn (October-December). The mean values for each season are calculated from the daily averages. The mean seasonal values and standard deviations of AOD(440) and $\alpha_{440\text{-}870}$ are shown in Figure 4. One of the main characteristic of the AOD(440) is its high variability, as indicated by the standard deviations in Figure 4a (the AOD variability is higher for shorter wavelengths, not shown here). The second main feature of the AOD is the very clear annual cycle with a large value in summer/spring and low value in autumn/winter. The maximum AOD found at Évora in spring is due to an exceptionally strong Saharan dust outbreak over southern Portugal from 4 to 9 April 2011 (Preiβler et al., 2011, Valenzuela et al., 2017) reaching values up to approximately 0.84, which explains why the mean value of AOD is higher than the median value (0.13 and 0.10, respectively). Another exceptional event that influenced the variability in the AOD was the aerosol plume from the

Eyjafjallajökull volcano in Iceland that reached the Iberian Peninsula (e.g., Sicard et al., 2012; Navas-Guzmán et al., 2013). The larger differences in the AOD between the coastal places and remote locations are observed in summer. The large values of the AOD recorded in summer with respect to the other seasons are explained by several reasons. The intense atmospheric convective dynamics prevailing under summer conditions, joined with the soil aridity during this period, provide a high mineral-dust loading to the atmosphere from the local soils (Pérez-Ramírez et al., 2012). At the same time, forest fires represent an additional source of aerosol particles during summer (Preißler et al., 2011; Pereira et al., 2014; Obregón et al., 2015). On the other hand, the lower values of the AOD during the autumn and winter seasons are due to the washing out of aerosols by rain, which is more frequent in these seasons. The high AOD values in summer found at Barcelona, Burjassot and Málaga are typical for the urban polluted sites with high emissions by road traffic, especially Barcelona (Reche et al., 2011). Coastal areas in the Iberian Peninsula can double their population during summer, which contributes to an increase in anthropogenic emissions. Additionally, in summer, Barcelona and Burjassot have a higher number of cruise ships for tourists in Spain, which is a significant source of emissions of atmospheric pollutants that are very often transported inland by the sea breeze.

A high variability is observed in $\alpha_{440-870}$, as indicated by the large standard deviation, revealing the presence of aerosols with different size distributions (Figure 4b). The $\alpha_{440-870}$ values do not generally present a remarkable seasonal cycle (except for Granada and Málaga), with only slightly lower values obtained in summer (opposite to the AOD behaviour). Therefore, we cannot conclude important changes in the particle size predominance among the seasons. The $\alpha_{440-870}$ seasonal patterns in Granada and Málaga are explained by more intense anthropogenic emissions in winter and by the

dryness of the terrain in the south of the Iberian Peninsula and the more frequent arrival of the Saharan dust in summer. It is worth noting that Barcelona and Burjassot sites present larger $\alpha_{440-870}$ values, therefore suggesting more predominance of fine particles that are probably associated with anthropogenic emissions. Stations located in southern sites present lower values of $\alpha_{440-870}$, which is explained by more contribution of dust particles from the Saharan dust outbreaks. Similar results (not shown here) have been obtained for the FMF with lower values for all sites in summer.

3.1.2. Particle size distribution

Figure 5 shows mean PSDs for each site. Two distinct modes are clearly identified for all sites: one corresponding to fine particles (with a mode radius near 0.5 μm) and another one corresponding to coarse particles (mode radius approximately 3 μm), with the contribution of each mode varying with the season. All sites have an almost similar volume concentration for the fine mode and the difference is found for the coarse mode. Málaga presents the highest PSD in the coarse mode followed by Huelva and Granada, with volume concentration mean values of 0.057, 0.052 and 0.047 $\mu m^3 \mu m^{-2}$, respectively. These values are almost three times larger than the values corresponding to the fine mode (0.020 $\mu m^3 \mu m^{-2}$). The value obtained from the coarse mode at Évora duplicates the value of the fine mode. However, Barcelona has essentially the same volume concentration for both modes.

The seasonal analysis reveals a different aerosol mixture, depending on the season and site (Figure 6 and Table 2). Barcelona does not present clear differences among the seasons, with negligible differences in the volume concentration for both modes. Granada presents a great difference among the seasons, with higher differences in the volume concentration between both modes in summer (0.018 $\mu m^3 \mu m^{-2}$ and 0.069

$\mu m^3 \mu m^{-2}$ for the fine and coarse modes, respectively). The median radius for the fine

mode in winter season varies between 0.15 μm for the southern sites and 0.18 ± 0.02

μm at Burjassots and in summer is essentially the same at all sites. For the coarse mode

in winter, the median radius varies from 1.9 ± 0.6 μm at Huelva to 2.4 ± 0.7 μm at

Barcelona and in summer from 1.8 to 2.1 μm. Changes within the fine mode radii and

volume are associated with differences in the aerosol properties and with different

processes such as aerosol aging (e.g., Pérez-Ramírez et al., 2012, 2017), aerosol

hygroscopic growth (e.g., Schafer et al., 2008; Eck et al., 2014), aerosol-cloud

interaction and new particle formation (e.g., Eck et al., 2012, 2014). On the other hand,

Cáceres, Évora, Huelva and Málaga show a displacement to the right of the coarse mode

radius and lower volumes during the cold seasons. Several shortcomings in the coarse

mode retrievals induce very large errors, close to 100%, for very large particles (e.g.,

Dubovik et al., 2000) and it is difficult to make further considerations about the

differences found. Nevertheless, the very large differences in the coarse mode could

indicate some differences in these particles.

3.1.3. Single scattering albedo

Using ω_o AERONET Level 2.0 data, there were very few available data for

temporal analyses. Indeed, we used Level 1.5 (cloud screened data with pre and post

calibrations applied) for ω_o temporal evolutions but following the same restrictions for

Level 2.0 for scattering angles and using only retrievals with AOD(440) > 0.15. This

approach is obviously a compromise between the data amount/quality and has been

previously adopted by other authors using the AERONET absorption data (e.g., Mallet

et al., 2013; Mateos et al., 2014, Valenzuela et al., 2017).

Table 3 shows a statistical summary of the daily mean values for ω_0. There are no important differences among the stations (a maximum in Barcelona and Huelva close to 0.94 and a minimum in Granada close to 0.90 at 675 nm) nor among the wavelengths (spectral difference close to 0.01, which is within the uncertainties of the retrievals). The values reported in this study agree with those reported by Mallet et al. (2013) for many European countries. The maximum values registered in all the sites are close to 1.0, which indicates that all the stations recordered events of non-absorbing aerosols. However, there are differences when studying the minimum values among stations: Huelva presents a minimum approximately 0.80 and Granada approximately 0.81. The influence of strong pollution events with a high contribution of carbonaceous species could explain these values. No remarkable seasonal pattern is observed, but the lowest minimum is registered in Granada, particularly in winter (0.87 ± 0.07). Although anthropogenic emissions in Granada are lower than in larger cities, such as Barcelona or Málaga, the orographic characteristics of Granada, placed in a valley surrounded by high altitude mountains, favours stagnation episodes in winter, which then favour an increasing accumulation of high absorbing aerosols originated by domestic heating and road traffic (Lyamani et al., 2012). Finally, Cáceres, Évora and Huelva present the lowest amount of ω_o data points because these places presented the lowest AOD and therefore less data fulfilling the restriction of $AOD_{440} > 0.15$ for the retrieval of ω_o.

Figure 7 presents the seasonal averages of $\omega_0(440)$ for the studied stations. Again, differences among the stations are very low (within ± 0.04). The most remarkable is the lack of a seasonal pattern for any station, which, combined with the information from AOD and PSD, yields important conclusions. For the southern locations, the frequent arrival of Saharan dust outbreaks in summer with the consequent increase of coarse particles is responsible for the relatively high absorption at 440 nm.

In winter, however, the absorbing aerosols are associated with pollution episodes. However, during the summer season in the northern locations, Saharan dust outbreaks are less frequent than in the south and anthropogenic pollution is responsible for aerosol absorption. The locations of Huelva, Évora and Cáceres present sporadic episodes of aerosol absorption, which is mostly associated with the transport of the Saharan dust and/or with the transport of anthropogenic pollution from industrial areas in the Iberian Peninsula. This sporadicity is explained by the low amount of single scattering albedo retrievals.

Further information about the aerosol type can be inferred by analysing the spectral dependence of ω_0 (e.g., Schuster et al., 2016a, b). The spectral difference in ω_0 is an indicator of the relative magnitude of the total aerosol absorption that occurs due to iron oxides in the mineral dust versus BC in the fine mode aerosols (Derimian et al., 2008; Eck et al., 2010). Positive values of $\Delta\omega_0$ are typical of anthropogenic pollution and biomass-burning, while negative $\Delta\omega_0$ are typical of dust particles (Dubovik et al., 2002). Figure 8 shows $\Delta\omega_0$, defined here as $\omega_o(440)-\omega_o(1020)$, for each site and for every season. As can be seen, during spring/summer $\Delta\omega0$ is negative at Évora, Granada and Málaga, suggesting the presence of dust that agrees with our analyses in sections 3.1.1 and 3.1.2.

3.2. Aerosol typing based on the aerosol optical properties

As discussed in section 3.1, the Iberian Peninsula presents large variability in aerosol particles among the different stations. In this section we analyse the combination of several properties to perform an aerosol typing.

3.2.1. Aerosol typing based on AOD and $\alpha_{440-870}$

Based on the AOD and $\alpha_{440-870}$ features of the different aerosol types, several authors have proposed a correlation between these parameters to discriminate the main aerosol types (e.g., Pace et al., 2006, Estellés et al., 2007, Toledano et al., 2007). Other authors (e.g., Pawar et al., 2015) have included the air-mass trajectory to consider the dominant airflow patterns. However, these studies suggest different AOD and $\alpha_{440-870}$ thresholds, which are site-dependent. Particles from different sources have different optical and radiative properties. Desert dust events are characterized by high values of AOD and low values of $\alpha_{440-870}$, while the situations dominated by urban and biomass burning particles are characterized by high values of $\alpha_{440-870}$ and variable AOD values (Dubovik et al., 2002, Pace et al., 2006, Toledano et al., 2007). Clean maritime conditions are characterized by low values of $\alpha_{440-870}$ and AOD(440) (Dubovik et al., 2002; Pace et al., 2006). Here, the classification proposed by Mateos et al. (2014) for the entire Iberian Peninsula is used. Thus, we have considered four categories, namely maritime (AOD(440) < 0.20 and $\alpha_{440-870}$ < 1), desert dust (AOD(440) > 0.20 and $\alpha_{440-870}$ < 1), continental clean (AOD(440) < 0.20 and $\alpha_{440-870}$ > 1), and continental polluted (AOD(440) > 0.2 and $\alpha_{440-870}$ > 1). Figure 9 shows the distribution of $\alpha_{440-870}$ data points as a function of AOD(440) for each site, and Table 4 shows the relative frequency of occurrence of the different aerosol scenarios for every site according to this classification.

All sites present the continental clean category as the most frequent one, with higher occurrences at Cáceres and Évora (above 60%), and Huelva and Málaga with low values close to the maritime type. On the other hand, Barcelona and Burjassot present an important continental polluted contribution (34% and 27%, respectively), due to vehicular and ship traffic (e.g. Reche et al., 2011). Our results are in agreement with

Mateos et al. (2014), who concluded that (i) the continental clean particles are the main features in remote areas of the Iberian Peninsula, (ii) there is an important contribution of continental pollution in Barcelona, and (iii) Málaga, Granada and Huelva are largely affected by Saharan dust particles.

From Table 1 we showed that the highest value of the FMF is found at Cáceres (0.71 ± 0.18) and the lowest is found at Málaga (0.52 ± 0.15). However, the highest value of $\alpha_{440-870}$ found is at Barcelona (1.31 ± 0.32) although Cáceres presents the second highest value (1.28 ± 0.38). The lowest $\alpha_{440-870}$ at Málaga (0.93 ± 0.35) agrees with the lowest value for the FMF. In general, for all sites there is a good linear correlation between the FMF and $\alpha_{440-870}$ (not shown here) with the determination coefficient (R^2) above 0.84, except for Huelva where R^2 is 0.73. In fact, for two sites (Granada and Málaga) R^2 is higher than 0.94. However, the relationship between FMF and $\alpha_{440-870}$ presents a high dispersion for $\alpha_{440-870}$ values greater than 1, which implies that for a given $\alpha_{440-870}$ value there is a wide range of values for the FMF. This is largely the result of in the increase of the fine mode particle size and the reduction in the $\alpha_{400-870}$ magnitude, as fine mode particles grow by aging and/or hygroscopic growth (Eck et al., 2010). Thus, the sensitivity of the Angstrom exponent in determining the fine mode fraction decreases as the fine mode becomes dominant. Caution should be exercised in those situations when using the Angstrom exponent as the primary aerosol size parameter. The size of the fine mode particles themselves also contributes to a significant variation of the Angstrom exponent, which is evident at larger values of $\alpha_{440-870}$ (Eck et al., 2005). Therefore, it seems to be more convenient to consider FMF when assessing the size instead of $\alpha_{440-870}$ because the FMF provides quantitative information for each fine and coarse mode, whereas $\alpha_{440-870}$ is a qualitative indicator (Lee et al., 2010).

3.2.2. Aerosol typing based on ω_o and the FMF

Distinguishing different aerosol types is important when quantifying the dispersion against the absorption processes through ω_o. Thus, one alternative method to potentially classify aerosols is the combination of FMF (determining the contribution of fine modes particles to the total AOD) and ω_o (determining aerosol absorption/scattering properties), successfully used by Lee et al. (2010). In this line, following Lee et al. (2010), Srivastava et al. (2012) used an approach to infer major aerosol types over the Indo-Gangetic Basin from ground-based sunphotometer measurements that were based on the combination of the particle size and absorption/scattering information. Amiridis et al. (2011) employed this scheme also besides the lidar ratio. Lee et al. (2010) distinguished absorbing/non-absorbing aerosols in terms of $\omega_o(440)$. This classification method is simple and robust, but its performance depends on thresholds. Thus, these authors considered four classes: Dust (FMF < 0.4 and $\omega_o(440)$ < 0.95), Mixture (0.4 < FMF < 0.6, independent of $\omega_o(440)$, absorbing fine (AF) (FMF > 0.6 and $\omega_o(440)$ < 0.95), and non-absorbing fine mode aerosols (NAF) (FMF > 0.6 and $\omega_o(440)$ > 0.95). Table 5 shows the relative frequency of occurrence for these four categories in each of the stations, including the mean values and standard deviations of AOD(440) and $\alpha_{440-870}$ for each aerosol type.

The most frequent aerosol type in Barcelona (50%) and Burjassot (48%) is AF, which is explained by the surrounding pollution sources to these stations. For Cáceres (41%) and Évora (37%), AF is also the most frequent aerosol type, but not as predominant as for the urban sites of Barcelona and Burjassot. The large influence of biomass-burning events during the study periods for these regions is the reason for the large influence of fine mode absorbing particles (e.g., Viana et al., 2013). In the

southern locations of Granada and Málaga, dust and mixed categories are the most frequent, which agrees with the large influence of Saharan dust outbreaks previously discussed in section 3.1.1. Nevertheless, both stations present a significant contribution of AF, which is explained by the peculiar characteristics of the sites: road traffic are important sources of particles in both places. Moreover, domestic heating is an important source in Granada (e.g., Lyamani et al., 2010) and ship traffic influences aerosol particle properties in Málaga (Valenzuela et al., 2014; Lyamani et al., 2010). Finally, the station in Huelva presents peculiarities when compared with the other stations: in Huelva no aerosol type is negligible, although dust and fine non-absorbing present almost double the frequency when compared with the other types (approximately 30% versus 15%). The large frequency of dust is explained by the proximity of the station to the Sahara desert, while the fine mode contribution can be associated with background particles, typically known as continental or remote. The presence of fine mode absorbing particles can be explained by the proximity to the industrial region of Rio Tinto (López et al., 2015).

Table 6 shows the relative frequencies of absorbing particles for the FMF parameter in the ranges: FMF > 0.6, FMF < 0.4 and 0.4 < FMF < 0.6. Absorbing aerosol is for $\omega_o(440)$ below to 0.95. We can observe that for FMF > 0.6 the aerosol particles are absorbing ones with a percentage above 60% (except Huelva). However, the largest percentages of FMF > 0.6 and absorbing aerosols are found in Granada and Huelva. If we assume that carbonaceous species are the main absorbers for FMF > 0.6, while sulphates are more associated with non-absorbing (e.g., Chin et al., 2002), these results could support the larger presence of carbonaceous species in Granada and Málaga. For Barcelona and Burjassot, the regions with largest AODs and FMF > 0.6,

the relative frequencies are approximately 60% absorbing and 40% non-absorbing, which is more typical for polluted cities near anthropogenic sources.

For FMF < 0.4, most of the cases are absorbing aerosols with percentages above 80%, except for Cáceres (47%) and Huelva (54%). In Granada and Málaga the percentage of absorbing aerosol is above 90%, which can be supported by assuming that the dust particles containing iron oxides act as the absorbing for particles with FMF < 0.4 (e.g., Chin et al., 2002). However, the results for Cáceres and Huelva, with percentages of absorbing aerosols of 47% and 54%, respectively, need further explanation. One reason for this could be the large errors in $\omega_o(440)$ for low AOD(440), in spite of the fact that we assumed the same limitations in the AERONET Level 2.0 scattering angles. Nevertheless, the large contribution of local sources of particles with FMF < 0.4 to the total aerosol load could be behind these low percentages of absorbing aerosols; e.g., sea salt in Huelva or re-suspended particles from the ground in Cáceres. Both of these types of particles can be assumed to be non-absorbing.

Finally, for the cases of a mixture of fine and coarse mode absorbing aerosols, the southern locations of Granada and Málaga have large percentages of absorbing aerosols, which suggests that these mixtures are mostly associated with carbonaceous (fine) and dust (coarse) particles, although discussions are not possible with only AERONET data. Barcelona and Burjassots, both at the north and very close to intense anthropogenic sources, also present a large contribution of mixture of absorbing aerosols, but with lowest percentages (approximately 80 %) than for Málaga and Granada. The larger presence of non-absorbing aerosols when the fine mode predominance was discussed before can cause these lower percentages of absorbing particles for mixtures. The remote places of Cáceres, Évora and Huelva present the lowest contributions of absorbing aerosols for mixtures. However, again we remark that

these places have the lowest AODs with larger induced errors in the retrievals of $\omega_o(440)$. Nevertheless, there could be many factors behind such as the influence of local sources; e.g., sea salt or continental aerosols.

Table 7 shows the relative frequency of the aerosol types based on the FMF and single scattering albedo (Dust, AF, NAF and a Mixture of cases) for each season and for each station. The same seasons as those in section 3.1.1 are used here. Barcelona and Burjassot do not present any remarkable seasonal pattern, always having the aerosol type of AF presenting the largest frequency. For these two stations, the maximum dust frequency is found in spring, which is expected due to the typical dust transport pattern for these stations (e.g., Pey et al., 2008; Estellés at al., 2007). Granada and Málaga present a very similar pattern between them, with a maximum of AF in winter and of dust in summer. This pattern is directly correlated with the seasonal pattern in the AOD and $\alpha_{400-870}$ obtained in section 3.1.1. Nevertheless, this pattern is different to the ones found in Barcelona and Burjassot. The differences in aerosol sources and in aerosol transport patterns for the Saharan dust explain the seasonal differences in aerosol types. For the remote stations (Cáceres and Évora), maximums in the AF are found in winter. The hypothesis behind this could be the use of domestic heating and road traffic because regions in the interior of the Iberian Peninsula present continental weather with cold winter. Both stations present very similar values of NAF between different seasons. Differences in the mixtures are found are typically correlated with an increase in the dust particles available for these mixtures. We note that Cáceres and Évora present a very similar pattern of Saharan dust transport and the differences for the seasonal pattern of dust between both stations can be explained by differences in the number of available measurements. Finally, Huelva presents the most complex seasonal pattern: only a minimum in the dust is found in autumn, which is explained by the

seasonal transport pattern of Saharan dust. Relative minimums of the AF are found in spring and summer while the opposite is found for NAF, which could be explained by differences in the anthropogenic sources that affect the regions. Nevertheless, these differences cannot be studied using only AERONET data.

3.2.3. Aerosol typing based on $\Delta\omega_o$ and FMF

Figure 10 shows $\Delta\omega_o$ ($\omega_o(440)$-$\omega_o(1020)$) against the FMF for each site, separating between categories for classifications 1 (with AOD(440) and $\alpha_{440-870}$) and 2 (with $\omega_o(440)$ and FMF), taking the different spectral pattern followed by ω_o into account, depending on the aerosol type. Figure 10 also includes the mean values and the standard deviations for ten bins (ranges 0-0.1, 0.1-0.2, 0.2-0.35, 0.5-0.6, 0.6-0.7, 0.7-0.8, 0.9-1.0). We have selected the extreme wavelengths because for all sites in general, $\omega(440)$ shows a very low variation with the FMF while $\omega(1020)$ clearly depends on the FMF. This result suggests that both coarse mode and fine mode aerosol mixtures have similar relative magnitudes of absorption relative to scattering at 440 nm. Similar results have been obtained by Eck et al. (2010) at Kanpur, India.

For all sites considering the classification using AOD and $\alpha_{440-870}$, we can observe a similar dependence for the categories classified as clean and polluted continental, showing a difference close to zero and positive for high values of the FMF. This dependence of ω_o, which decreases as the wavelength increases for a domain size range of predominately fine aerosols, is typical of urban aerosols, but there is no difference between both categories with overlapping categories. Additionally, the dust category presents cases with a positive $\Delta\omega_o$ and a range of sizes is not expected (FMF>0.4) because the domination of large particles in desert dust aerosol is the principal feature differentiating the optical properties of dust from the fine-mode

dominated biomass burning and urban-industrial aerosols (Dubovik et al., 2002). Additionally, the maritime category is included in the range of intermediate values for the FMF (between 0.4 and 0.6), which is not expected, because the dominant size is coarse (Dubovik et al., 2002). However, the second classification is more appropriate to distinguish between the differences in the aerosol types, showing significant dependences between categories, with $\Delta\omega_o > 0$ more marked for aerosols BC and $\Delta\omega_o < 0$ in the dust category.

On the other hand, we can observe that there is a clear relationship between $\Delta\omega_o$ and FMF, with values lower than zero for FMF below ~ 0.5, and thus, we found values greater than zero for values above that FMF threshold. This result implies that there are two different patterns depending on the predominance of coarse/fine particles in their contribution to the aerosol load. Thus, when the fine mode particles become dominant, ω_o decreases with an increasing wavelength, which is typical of anthropogenic aerosols (Dubovik et al., 2002). The increase in ω_o for the highest FMF values can be partly due to the increase in the fine mode particle radius, which increases the relative scattering efficiency. There is an opposite relation for aerosols with a predominance of coarse particles; increasing the FMF increases the absorption, which is a pattern typical of mineral dust aerosols. The difference between the places is the value of the FMF where the change in the sign of $\Delta\omega_o$ occurs.

The difference between ω_o at 440 nm and 1020 nm has two advantages: first, it is expected that the difference will provide a better accuracy than absolute values since the retrieval of its spectral dependence is more reliable than that of an absolute value; second, the spectral behaviour of an ω_o curve can be characterized by only one parameter ($\Delta\omega_o$). Negative values of $\Delta\omega_o$ will be related to a stronger absorption by dust at 440 nm, while positive values are related to a stronger absorption by BC containing

particles at 1020 nm. Consequently, Figure 10 classifies the spectral ω_o for events having dust- or pollution-dominated contributions and different degrees of mixing. From Figure 10, we can observe that there is a good relationship between $\Delta\omega_o$ and the FMF for all sites with R^2 above 0.90. The fitting equation is a two-degree polynomial relation as follows:

$$\Delta\omega_o = a + b\,FMF + c\,FMF^2 \qquad (1)$$

where a, b and c are fitting parameters. This relationship contains the spectral ω_o behaviour; however, the difference itself represents only relative values and gives no information about the absolute ω_o values. The ratio $\Delta\omega_o/\omega_o(440)$ carries information about the spectral ω_o as well as about the absolute values. Table 8 and Table 9 show these parameters and their uncertainties. For parameters a, b and c, in absolute terms the lowest values are found in Évora while the highest are found in Granada. The use of parameters a, b, and c and measurements of FMF using spectral AODs as inputs serve to infer columnar aerosol absorption properties, which is particularly useful when no measurements of sky radiance are available or when other conditions needed for retrievals are not fulfilled. In fact, a relationship among $\Delta\omega_o/\omega_o(440)$, the percentage of iron in the total particulate mass, and the pollution components was derived by Derimian et al. (2008) at Negev (Israel). They also studied the relationship between $\Delta\omega_o$ and $\alpha_{440-870}$, and found a similar dependence; as α increases from approximately 0 to approximately 1.5, the spectral ω_o gradually changes from a stronger absorption at 440 nm to a stronger absorption at 1020 nm. The difference $\Delta\omega_o$ shows negative values in response to the dominant iron contribution and gradually becomes positive as the role of BC increases.

4. Conclusions

In this work, columnar aerosol optical and microphysical properties obtained from AERONET were analysed for seven sites in the Iberian Peninsula (Barcelona, Burjassot, Cáceres, Évora, Granada, Huelva and Málaga) during the period of 2010-2012. The sites are representative of different aerosol types and sources as well as different atmospheric conditions. The results showed a clear seasonal pattern for the aerosol optical depth (AOD) for all stations with larger values in summer/spring and lower values in winter/autumn, while for the Angstrom parameter ($\alpha_{440-870}$) differences are observed among the stations. Although urban polluted areas such as Barcelona and Burjassot did not reveal important seasonal pattern in $\alpha_{440-870}$, the southern locations such as Granada, Málaga and Huelva presented a seasonal pattern with larger values in winter and lower values in summer. Such differences in $\alpha_{440-870}$ have been explained by differences in the aerosol sources. Although Saharan dust outbreaks are the most important source of natural aerosol in the Iberian Peninsula, they are more frequent and intense in the southern locations in summer. Northern areas present higher anthropogenic activity in summer, which explains the seasonal cycle in the AOD and the relative lack of seasonal variability in $\alpha_{440-870}$. Granada, however, presented seasonality in the anthropogenic activity with a maximum in winter, which explains the enhanced seasonal pattern in $\alpha_{440-870}$. Málaga and Huelva presented slight seasonal patterns due to intense anthropogenic activity in summer. Finally, Cáceres and Évora presented the lowest mean values of the AOD of the entire data set and also presented larger variability in the AOD and $\alpha_{440-870}$. The remote location of Cáceres and Évora explained these findings, allowing for these stations to be references of remote places.

Differences among the stations for aerosol size distribution (PSD) and single scattering albedo (ω_o) have also been found. Changes in the PSD are generally coherent with the patterns observed for the AOD and $\alpha_{440-870}$. Changes within the fine mode both

among stations and among seasons have been generally observed, but a deep analyses of these changes will require further evaluation with complementary in-situ measurements. Similarly, changes within the coarse mode have been observed but no further analysis were possible due to the large errors of the retrievals for very large particles. The temporal analysis of ω_o did not reveal important changes if errors are taken into account. Indeed, the analyses of ω_o indicate that aerosol absorption is mostly related to pollution events and to the presence of Saharan dust particles in the atmosphere. These events can affect the stations in different ways, depending on the local anthropogenic sources and on the locations; e.g., distance to the Saharan dust sources and/or distance to the pollution sources.

To face the problem of the sporadic AERONET measurements, particularly for ω_o, which requires completely clear skies, we have presented two different classifications to distinguish between aerosol types and a third new classification scheme is proposed. The first uses AOD and $\alpha_{440-870}$, only requiring spectral AODs measurements. The second is more complete and uses ω_o and the FMF. This second classification has been found to be more adequate but is more complex because it requires additional information from sky radiance measurements and of the use of retrieval techniques. According to this second classification we have found absorbing fine to be the more predominant category at Barcelona, Burjassot, Cáceres and Évora, while in Granada the more frequent category is Dust and at Málaga the Mixture. On the other hand, this work found a relationship between $\Delta\omega_o$ ($\omega_o(440)-\omega_o(1020)$) and the FMF with a determination coefficient above 0.90 for all sites. This relationship indicates a spectral ω_o for different aerosol types through the size. However, $\Delta\omega_o$ represents only relative values and gives no information about the absolute ω_o values. Alternatively, we have found a relationship between the ratio of $\Delta\omega_o$ to $\omega_o(440)$ and the

FMF because this ratio carries information about the spectral ω_o as well as about the absolute values. This relationship can be used as an alternative tool to distinguish between different aerosol types.

In this analysis of sites in the Iberian Peninsula, we found a similarity between different sites according to their geographical location; one cluster is located in the Eastern Iberian Peninsula (Barcelona and Burjassot), with Barcelona having more pollution than the other sites with values of AOD(440), $\alpha_{440-870}$, FMF and ω_o greater than those of Burjassot; the other cluster is located in the Western Iberian Peninsula (Cáceres and Évora). This group presents the lowest values of the AOD of all of the sites, with greater values of the parameters in Cáceres than Évora, except for ω_o. The last cluster, located in the southern Iberian Peninsula (Granada, Huelva and Málaga), presents a large predominance of coarse aerosols in comparison to the other groups and a higher frequency of dust events due to its proximity to the Saharan desert, although Huelva is different that Granada and Málaga, with a high proportion of fine non-absorbing aerosols.

References

Alados-Arboledas, L., Lyamani, H., and Olmo, F.J. 2003. Aerosol size properties at Armilla, Granada (Spain). Q.J.R. Meteorol. Soc. 129, 1395-1413.

Amiridis, V., Balis, B., Giannakaki, E., Kazadzis, S., Arola, A., Gerasopoulosawar, E., 2011. Characterization of the aerosol type measurements of the lidar ratio and the estimations of the single scattering albedo. Atmos. Res. 101, 46–53.

Bennouna, Y.S., Cachorro, V.E., Toledano, C., Berjón, A., Prats, N., Fuertes, D., Gonzalez, R., Rodrigo, R., Torres, B., de Frutos, A.M., 2011. Comparison of atmospheric aerosol climatologies over southwestern Spain derived from AERONET and MODIS. Remote Sens. Environ. 115, 1272-1284. https://doi.org/10.1016/j.rse.2011.01.011.

Boucher, O., Randall, D., Artaxo, P., Bretherton, C., Feingold, G., Forster, P., Kerminen, V.M., Kondo, Y., Liao, H., Lohmann, U., Rasch, P., Satheesh, S.K., Sherwood, S., Stevens, B., Zhang, X. Y., 2013. Clouds and aerosols, in: Climate Change 2013: The Physical Science Basis, Contribution of Working Group I to the Fifth Assessment Report of the Intergovernmental Panel on Climate Change, edited by: Stocker, T. F., Qin, D., Plattner, G.K., Tignor, M., Allen, S. K., Doschung, J., Nauels, A., Xia, Y., Bex, V., Midgley, P. M., Cambridge University Press. 571–657.

Chin, M., Ginoux, P., Kinne, S., Torres, O., Holben, BN., Duncan, BN., Martin RV., Logan, J.A., Higurashi, A., 2002. Tropospheric aerosol optical thickness from the

Gocart model and comparisons with satellite and Sun photometer measurements. J. Atmos. Sci. 59, 461-483.

Derimian Y., Karnieli, A. , Kaufman Y.J., Andreae, M.O., Andreae, T.W., Dubovik, O., Maenhaut, W., Koren, I., 2008. The role of iron and black carbon in aerosol light absorption. Atmos. Chem. Phys. 8, 3623–3637.

Dockery, D.W., Pope C,A., 1996. Epidemiology of acute health effects: summary of time-series, in: Particles in our air: concentration and health effects, edited by: Wilson, R. and Spengler, J. D., Harvard University Press, Cambridge, MA, USA. 123–147.

Dubovik, O., King M.D., 2000. A flexible inversion algorithm for retrieval of aerosol optical properties from Sun and sky radiance measurements. J. Geophys. Res. 105, 20673–20696.

Dubovik, O., Smirnov, A., Holben, B.N., King, M.D., Kaufman, Y.J., Eck, T.F., Slutsker, I., 2000. Accuracy assessments of aerosol optical properties retrieved from Aerosol Robotic Network (AERONET) Sun and sky radiance measurements. J. Geophys. Res. 105, 9791–9806.

Dubovik, O., Holben, B.N., Eck, T.F., Smirnov, A., Kaufman, Y.J., King, M,D., Tanré, D., Slutsker I., 2002. Variability of absorption and optical properties of key aerosol types observed in worldwide locations. J. Atmos. Sci. 59, 590–608.

Dubovik, O., Sinyuk, A., Lapyonok, T., Holben, B.N., Mishchenko, M., Yang, P., Eck, T.F., Volten, H., Muñoz, O., Veihelmann, B., van der Zande, W.J., Leon, J.F., Sorokin, M., Slutsker, I., 2006. Application of spheroid models to account for aerosol particle nonsphericity in remote sensing of desert dust. J. Geophys. Res. 111, D11208, DOI: 10.1029/2005JD006619.

Eck, T., Holben, B., Reid, J., Dubovik, O., Smirnov, A., O'Neill, N., Slutsker, I., Kinne, S., 1999. Wavelength dependence of the optical depth of biomass burning, urban and desert dust aerosols. J. Geophys. Res. 104, 333–349.

Eck, T.F., Holben, B.N., Dubovik, O., Smirnov, A., Goloub, P., Chen, H.B., Chatenet, B., Gomes, L., Zhang, X.Y., Tsay, S.C., Ji, Q., Giles, D., Slutsker I., 2005. Columnar aerosol optical properties at AERONET sites in central eastern Asia and aerosol transport to the tropical mid-Pacific. J. Geophys. Res. 110, D06202, DOI:10.1029/2004JD005274.

Eck, T., Holben, B.N., Sinyuk, A., Pinker, R., Goloub, P., Chen, H., Chatenet, B., Li, Z., Singh, R.,Tripathi, S., Reid, J., Giles, D., Dubovik, O., O'Neill, D., Smirnov, A., Wang, P., Xia, X., 2010. Climatological aspects of the optical properties of fine/coarse mode aerosol mixtures. J. Geophys. Res. 115, D19205, DOI:10.1029/2010JD014002.

Eck, T.F., Holben, B.N., Reid, J.S., Giles, D.M., Rivas, M.A., Singh, R.P., Tripathi, S.N., Bruegge, C.J., Platnick, S., Arnold, G.T., Krotkov, N.A., Carn, S.A., Sinyuk, A., Dubovik, O., Arola, A., Schafer, J.S., Artaxo, P., Smirnov, A., Chen, H., Goloub, P., 2012. Fog- and cloud-induced aerosol modification observed by the Aerosol Robotic Network (AERONET), J. Geophys. Res. 117, D07206, DOI:10.1029/2011JD016839.

Eck, T.F., Holben, B.N., Reid, J.S., Arola, A., Ferrare, R.A., Hostetler, C.A., Crumeyrolle, S.N., Berkoff, T.A., Welton, E.J., Lolli, S., Lyapustin, A., Wang, Y., Schafer, J.S., Giles, D,M., Anderson, B.E., Thornill, K.L., Minnis, P., Pickering, K.E., Loughner, C.P., Smirnov, A., Sinyuk, A., 2014. Observations of rapid aerosol optical depth enhancements in the vicinity of polluted cumulus clouds, Atmos. Chem. Phys. 14, 11633-11656.

Elias, T., Silva, A.M., Belo, N., Pereira, S., Formenti, P., Helas, G., Wagner, F., 2006. Aerosol extinction in a remote continental region of the Iberian Peninsula during summer. J. Geophys. Res. 111, D14204: 1–20, DOI:10.1029/2005JD006610.

Estellés, V., Martínez-Lozano, J.A., Utrillas, M.P., Campanelli, M., 2007. Columnar aerosol properties in Valencia (Spain) by ground based sun photometry. J. Geophys. Res. 112(D11201): 1–9, DOI: 10.1029/2006JD008167.

Giles, D.M., Sinyuk, A., Sorokin, M.S., Schafer, J.S., Smirnov, A., Slutsker, I., Eck, T.F., Holben, B.N., Lewis, J., Campbell, J., Welton, E.J., Korkin, S., Lyapustin, A., 2018. Advancements in the Aerosol Robotic Network (AERONET) Version 3 Database – Automated Near Real-Time Quality Control Algorithm with Improved Cloud Screening for Sun Photometer Aerosol Optical Depth (AOD) Measurements. Atmos. Meas. Tech. Discuss., https://doi.org/10.5194/amt-2018-272

Holben, B.N., Eck, T.F., Slutsker, I., Tanre, D., Buis, J.P., Setzer, K.A., Vermote, E., Reagan, J.A., Kaufman, Y.J., Nakajima, T., Lavenu, F., Jankowiak, I., Smirnov, A., 1998. AERONET - A Federated Instrument Network and Data Archive for Aerosol Characterization. Rem. Sens. Environ. 66(1), 1–16.

Horvath, H., 1995. Estimation of the average visibility in central Europe, Atmos. Environ. 29: 241-246.

Kampa, M., Castanas, E., 2008. Human health effects of air pollution. Envir. Pollu. 151, 362-367. DOI:10.1016/j.envpol.2007.06.012.

Lee, J., Kim, J., Song, C.H., Kim, S.B., Chun, Y., Sohn, B.J., Holben, B.N., 2010. Characteristics of aerosol types from AERONET sunphotometer measurements. Atmos. Environ. 44, 3110–3117, DOI:10.1016/j.atmosenv.2010.05.035.

López, J.F., Cachorro, V.E., de Frutos, A.M., 2015. Analysis of aerosol scattering properties measured by a nephelometer at a coastal-rural site in the Atlantic

southwest of the Iberian Peninsula. J. of Atmos. and Solar-Terrestrial Phys. 132, 48-63.

Lyamani, H., Olmo ,F.J., Alcántara, A., Alados-Arboledas, L., 2006a. Atmospheric aerosols during the 2003 heat wave in southeastern Spain I: spectral optical depth. Atmos. Environ. 40, 6453–6464, DOI:10.1016/j.atmosenv.2006.04.048.

Lyamani, H., Olmo, F.J., Alcántara, A., Alados-Arboledas, L., 2006b. Atmospheric aerosols during the 2003 heat wave in southeastern Spain II: microphysical columnar properties and radiative forcing. Atmos. Environ. 40, 6465–6476, DOI: 10.1016/j.atmosenv.2006.04.047.

Lyamani, H., Olmo, F.J., Alados-Arboledas, L., 2010. Physical and optical properties of aerosols over an urban location in Spain: Seasonal and diurnal variability, Atmos. Chem. Phys. 10, 239–254, DOI:10.5194/ acp-10-239-2010.

Lyamani, H., Olmo, F.J., Foyo, I., Alados-Arboledas, L., 2011. Black carbón aerosols over an urban área in south-eastern Spain: changes detected after the 2008 economic crisis. Atmos. Environ, 6423–6432.

Lyamani, H., Fernández-Gálvez, J., Pérez-Ramírez, D., Valenzuela, A., Antón, M., Alados, I., Titos, G., Olmo, F.J., Alados-Arboledas, L., 2012. Aerosol properties over two urban sites in South Spain during an extended stagnation episode in winter season. Atmos. Environ. 62, 424-432.

Lyamani, H., Valenzuela, A., Pérez-Ramírez, D., Toledano, C., Granados-Muñoz, M.J., Olmo, F.J., Alados-Arboledas, L., 2015. Aerosol properties over the western Mediterranean basin: temporal and spatial variability, Atmos. Chem. and Phys. 15, 2473-2486.

Mallet, M., Dubovik, O., Nabat, P., Dulac, F., Kahn, R., Sciare, J., Paronis, D., Léon, J.F., 2013. Absorption properties of Mediterranean aerosols obtained from multi-year

ground-based remote sensing observations, Atmos. Chem. Phys. 13, 9195–9210, DOI:10.5194/acp-13-9195-2013.

Markowicz, K.M., Flatau, P.J., Ramana, M.V., Crutzen, P.J., Ramanathan, V., 2002. Absorbing mediterranean aerosols lead to a large reduction in the solar radiation at the surface, Geophys. Res. Letters 29 (20), 1–4, DOI:10.1029/2002GL015767.

Mateos, D., Sanchez-Lorenzo, A., Antón, M., Cachorro, V.E., Calbó, J., Costa, M.J., Torres, B., Wild, M., 2014. Quantifying the respective roles of aerosols and clouds in the strong brightening since the early 2000s over the Iberian Peninsula, J. Geophys. Res. Atmos. 11, 10382–10393, DOI:10.1002/2014JD022076.

Mateos, D., Cachorro, VE., Toledano, C., Burgos, M.A., Bennouna, Y., Torres, B., Fuertes, D., González, R., Guirado, C., Calle, A., de Frutos, A.M., 2015. Columnar and surface aerosol load over the Iberian Peninsula establishing annual cycles, trends, and relationships in five geographical sectors, Sci. of the Total Environ. 1518-519, 378-392.

Navas-Guzmán, F., Müller, D., Bravo-Aranda, J.A., Guerrero-Rascado, J.L., Granados-Muñoz, M.J., Pérez-Ramírez, D., Olmo, F.J., Alados-Arboledas, L., 2013. Eruption of the Eyjafjallajökull Volcano in spring 2010: Multiwavelength Raman lidar measurements of sulphate particles in the lower troposphere, J. of Geophys. Res. Atmos. 118, 1804-1813.

Obregón, M.A., Serrano, A., Cancillo, M.L., 2009. Aplication of different classifications to aerosols in column at Cáceres, paper presented at 6º Simpósio de Meteorologia e Geofisica da APMG/10º Encontro Luso-Espanhol de Meteorologia, Caparica, Portugal.

Obregón,M.A., Serrano, A., Cancillo, M.L., Cachorro, V.E., Toledano C., 2015. Aerosol radiometric properties at Western Spain (Cáceres station). Int. J. Climatol. 35, 981–990. DOI: 10.1002/joc.4031.

O'Neill, N. T., Eck, T.F., Smirnov, A., Holben, B.N., Thulasiraman, S., 2003. Spectral discrimination of coarse and fine mode optical depth, J. Geophys. Res., 108(D17), 4559, DOI:10.1029/2002JD002975.

Pace, G., di Sarra, A., Meloni, D., Piacentino, S., Chamard, P., 2006. Aerosol optical properties at Lampedusa (Central Mediterranean). Influence of transport and identification of different aerosol types, Atmos. Chem. Phys. 6, 697–713, DOI:10.5194/acp-6-697-2006.

Papadimas, C.D., Hatzianastassiou, N., Matsoukas, C., Kanakidou, M., Mihalopoulos, N., Vardavas, I., 2012. The direct effect of aerosols on solar radiation over the broader Mediterranean basin. Atmos. Chem. Phys. 12, 7165-7185, DOI:10.5194/acp-12-7165-2012.

Patron, D., Lyamani, H., Titos, G., Casquero-Vera, J.A., Cardell, C., Močnik, G., 2017.
Monumental heritage exposure to urban balck carbon pollution. Atmos. Env. 170, 22-32.

Pawar ,G.V., Devara, P.C.S., Ahar, G.R., 2015. Identification of aerosol types over an urban site based on air-mass trajectory classification. Atmos. Res. 164-165, 142–155.

Pereira, S.N., Preibler, J., Guerrero-Rascado, J.L., Silva, A.M., Wagner, F., 2014. Forest fire smoke layers observed in the free troposphere over Portugal with a multiwavelength Raman lidar: Optical and microphysical properties, The Scientific World Journal, ID 421838. DOI: 10.1155/2014/421838, 1-11, 2014.

Pérez, N., Pey, J., Reche, C., Cortés, J., Alastuey, A., Querol, X., 2016. Impact of harbour emissions on ambient PM10 and PM2.5 in Barcelona (Spain): evidences of secondary aerosol formation within the urban area. Sci. Total Environ. 571, 237–250.

Pérez-Ramírez, D., Lyamani, H., Olmo, F.J, Whiteman, D.N., Alados-Arboledas, L., 2012. Columnar aerosol properties from sun-and-star photometry: statistical comparisons and day-to-night dynamic. Atmos. Chem. Phys. 12, 9719–9738, DOI:10.5194/acp-12-9719-2012.

Pérez-Ramírez, D., Lyamani, H., Smirnov, A., O´Neill, N.T., Veselovskii, I., Whiteman, D.N., Olmo, F.J., Alados-Arboledas, L., 2016. Statistical study of day and night hourly patterns of columnar aerosol properties using sun and star photometry, Proceedings of SPIE, 10001, 10001K-1 – 10001K-18.

Pérez-Ramírez, D., Andrade-Flores, M., Eck, T.F., Stein, A.F., O´Neill, N.T., Lyamani, H., Gassó, S., Whiteman, D.N., Veselovskii, I., Velarde, F., Alados-Arboledas, L., 2017. Multi year aerosol characterization in the tropical Andes and in adjacent Amazonia using AERONET measurements, Atmos. Environ. 166, 412-432.

Pey, J., Rodríguez, S., Querol, X., Alastuey, A., Moreno, T., Putaud, J.P., Van Dingenen, R., 2008. Variations of urban aerosols in the Westren Mediterranean. Atmos. Environ. 42, 9052-9062.

Prats, N., Cachorro, V.E., Sorribas, M., Mogo, S., Berjon, A., Toledano, C., de Frutos, A.M., de la Rosa, J., Laulainen, N., de la Morena, B.A., 2008. Columnar aerosol optical properties during "El Arenosillo 2004 summer campaign". Atmos. Environ. 42, 2643–2653.

Preißler, J., Wagner, F., Pereira, S.N., Guerrero-Rascado, J.L., 2011. Multi-instrumental observation of an exceptionally strong Saharan dust outbreak over Portugal, J. Geophys. Res. 116, D24204, DOI:10.1029/2011JD016527.

Queface, A.J, Piketh, S.J, Eck, T.F, Tsay, S.C., Mavume, A.F., 2011. Climatology of aerosol optical properties in Southern Africa. Atmos Environ. 45, 2910–2921. DOI: 10.1016/j.atmosenv.2011.01.056.

Reche, C., Viana, M., Moreno, T., Querol, X., Alastuey, A., Pey, J., Pandolfi, M., Prèvôt, A., Mohr, C., Richard, A., Artiñano, B., Gomez-Moreno, F.J., Cots, N., 2011. Peculiarities in atmospheric particle number and size-resolved speciation in an urban area in the western Mediterranean: Results from the DAURE campaign, Atmos. Environ. 45, 5282–5293, DOI:10.1016/j.atmosenv.2011.06.059.

Sicard, M., Guerrero-Rascado, J.L., Navas-Guzmán, F., Preibler, J., Molero, F., Tomás, S., Bravo-Aranda, J.A., Comerón, A., Rocadenbosch, F., Wagner, F., Pujadas, M., Alados-Arboledas, L., 2012. Monitoring of the Eyjafjallajökull volcanic aerosol plume over the Iberian Peninsula by means of four EARLINET lidar stations, Atmos. Chem. Phys. 12, 3115-313.

Silva, A.M., Bugalho, M.L., Costa, M.J., von Hoyningen-Huene, W., Schmidt, T., Heintzenberg, J., and Henning, S., (2002). Aerosol optical properties from columnar data during the second Aerosol Characterization Experiment on the south coast of Portugal. J. Geophys. Res. Atmos., 107, Nº 22, 4642.

Schafer, J.S., Eck, T.F., Holben, B.N., Artaxo, P., Duarte, A.F., 2008. Characterization of the optical properties of atmospheric aerosols in Amazonia from long-term AERONET monitoring (1993-1995 and 1999-2006), J. Geophys. Res. 113, D04204.

Schuster, G.L., Dubovik, O., Holben, B.N., 2006. Angstrom exponent and bimodal aerosol size distributions. J. Geophys. Res. 111, D07207. DOI:10.1029/2005JD006328.

Schuster, G.L., Dubovik, O., Arola, A., 2016 a. Remote sensing of soot carbon – Part 1: Distinguishing different absorbing aerosol species, Atmos. Chem. Phys. 16, 1565–1585, DOI: 10.5194/acp-16-1565-2016.

Schuster, G.L., Dubovik, O., Arola, A., Eck, T.F., Holben, B.N., 2016 b. Remote sensing of soot carbon – Part 2: Understanding the absorption Ångström exponent, Atmos. Chem. Phys. 16, 1587–1602, DOI: 10.5194/acp-16-1587-2016.

Schwartz, J., 1994. Air pollution and daily mortality: a review and metaanalysis. Environ. Res. 64, 36–52.

Smirnov, A., Holben, B.N., Eck, T.F., Dubovik, O., Slutsker, I., 2000. Cloud screening and quality control algorithms for the AERONET data base, Remote Sens. Environ. 73, 337–349.

Srivastava, A.K., Tripathi, S.N., Sagnik, D., Kanawade, V.P., Tiwari, S., 2012. Inferring aerosol types over the Indo-Gangetic Basin from ground based sunphotometer measurements, Atmos. Res. 109-110, 64–75.

Titos, G., Ealo, M., Pandolfi, M., Pérez, N., Sola, Y., Sicard, M., Comerón, A., 2017. Spatiotemporal evolution of a severe winter dust event in the western Mediterranean: Aerosol optical and physical properties. J. Geophys. Res. Atmos. 122 (7), 4052-4069.

Toledano, C., Cachorro, V.E., Berjón, A., de Frutos, A.M., Sorribas, M., de la Morena, B., Goloub P. 2007. Aerosol optical depth and Ångström exponent climatology at El Arenosillo AERONET site (Huelva, Spain). Q. J. R. Meteorol. Soc. 133, 795–807, DOI: 10.1002/qj.54.

Valenzuela, A., Olmo, F.J., Lyamani, H., Granados-Muñoz, M.J., Antón, M., Guerrero-Rascado, J.L., Quirantes, A., Toledano, C., Pérez-Ramírez, D., Alados-Arboledas, L., 2014. Aerosol transport over the western Mediterranean basin: Evidence of the

contribution of fine particles to desert dust plumes over Alborán Island, J. Geophys. Res. Atmos. 119, 14028-14044.

Valenzuela, A., Costa, M.J., Guerrero-Rascado, J.L., Bortoli, D., Olmo, F.J., 2017. Solar and thermal radiative effects during the 2011 extreme desert dust episode over Portugal, Atmos. Environ. 148, 16-29.

Viana, M., Reche, C., Amato, F., Alastuey, A., Querol, X., Moreno, T., Lucarelli, F., Nava, S., Calzolai, G., Chiari, M., Rico, M., 2013. Evidence of biomass burning aerosols in the Barcelona urban environment during winter time, Atmos. Environ. 72, 81-88.

Wagner, F., Silva, A.M., 2018. Some considerations about Ångström exponent distributions, Atmos. Chem. Phys. 8, 481–489.
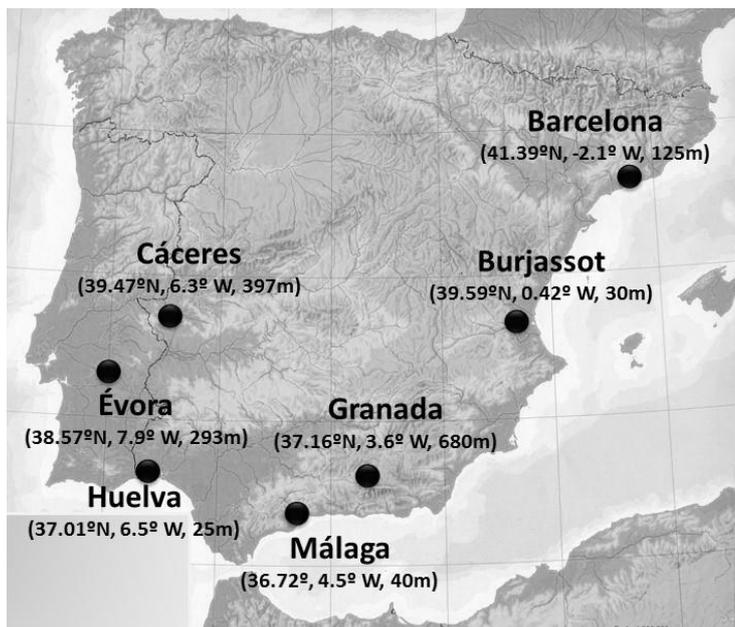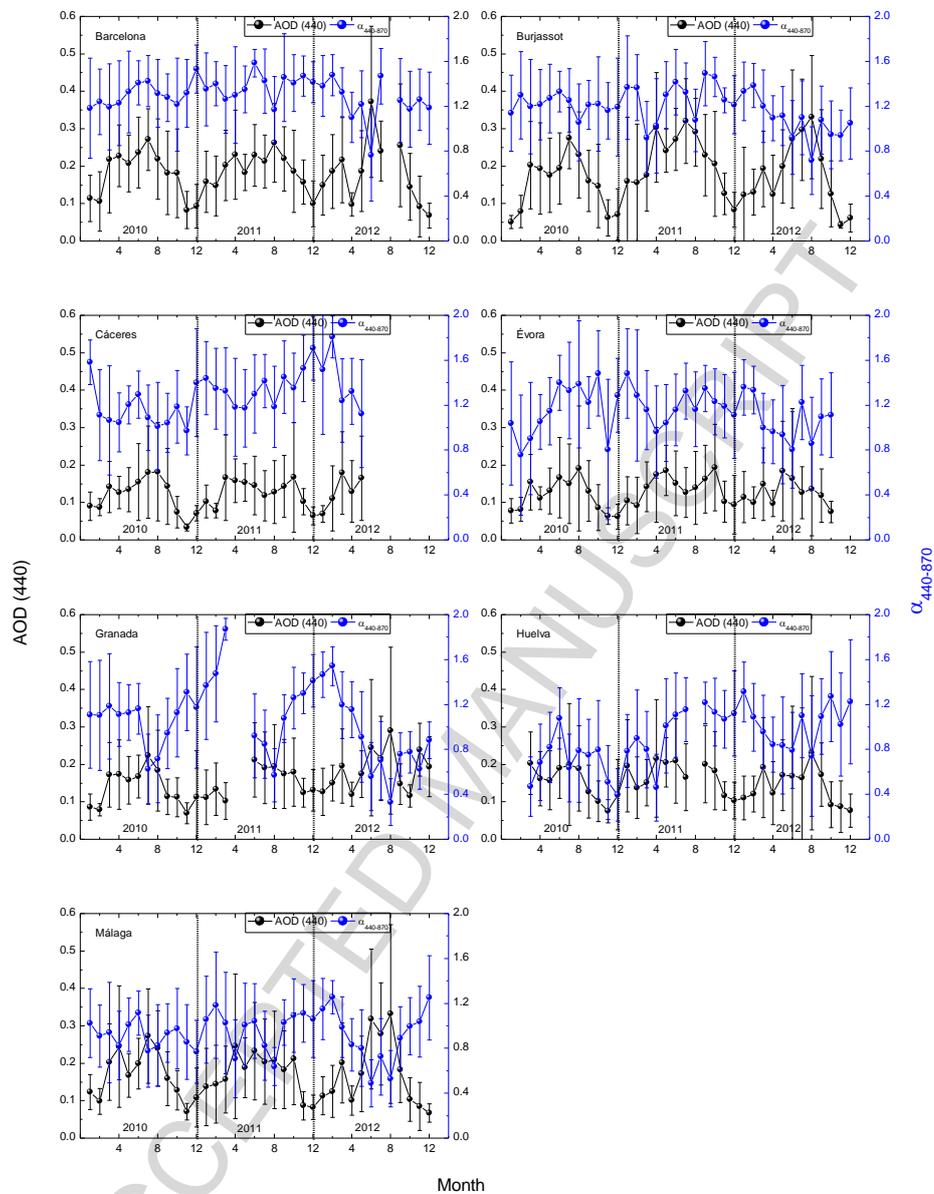
Figure 1. Location of the AERONET sites used in this work.

Figure 2. Annual cycle of AOD at 440 nm and mean monthly α between 440 and 870 nm for every site in 2010-2012. Bars denote one standard deviation.
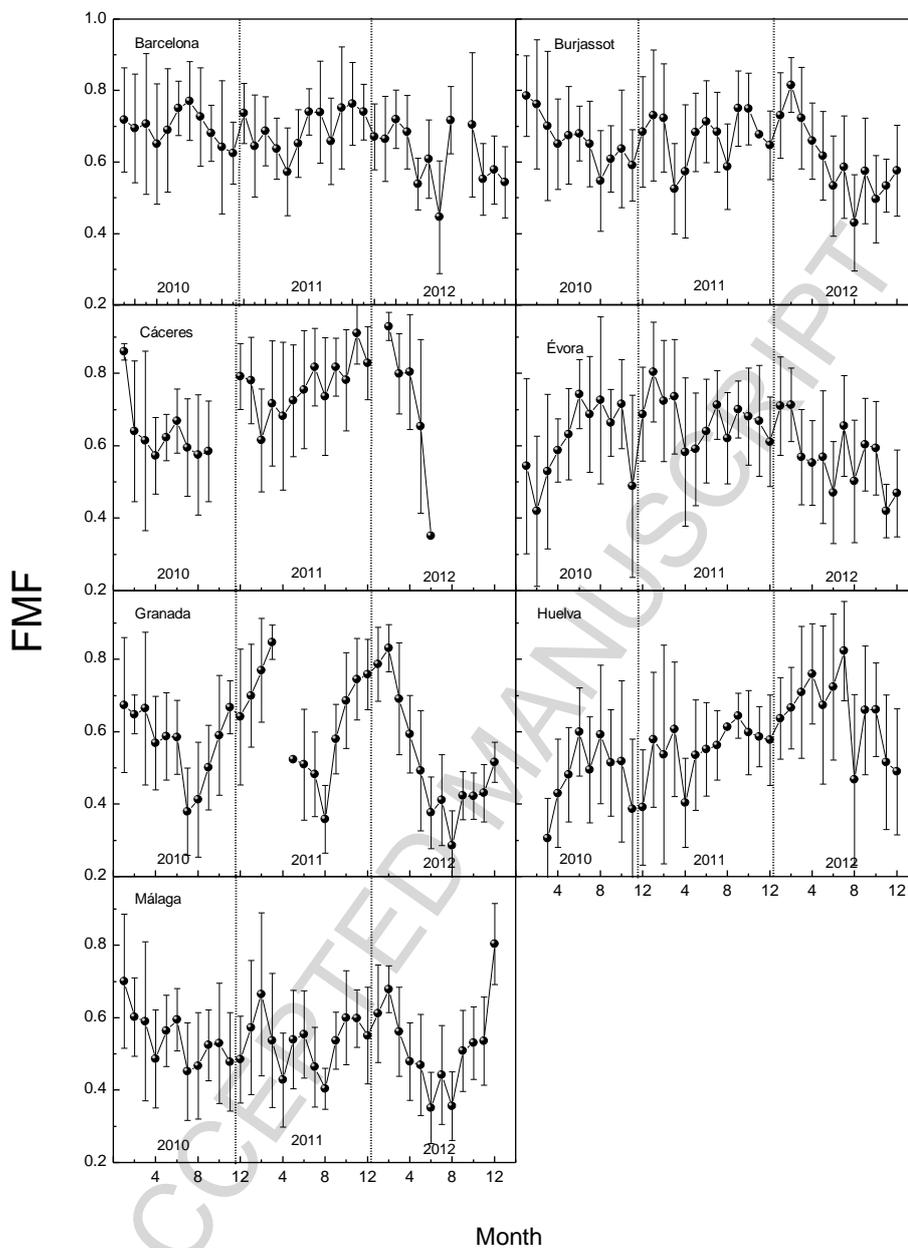
Figure 3. Annual cycle of mean monthly FMF for every site in 2010-2012. Bars denote one standard deviation.
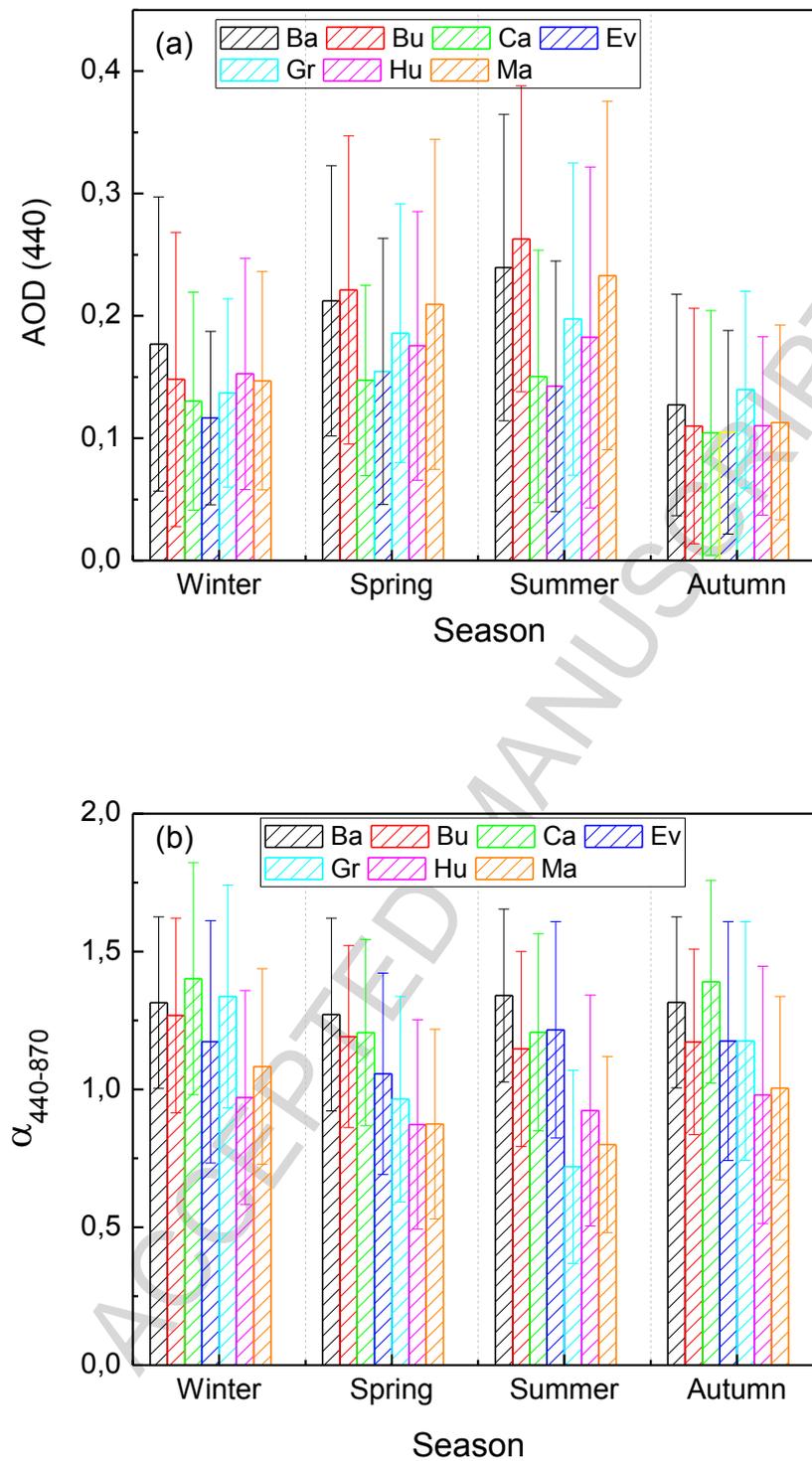
Figure 4: Seasonal dependence of: (a) AOD at 440 nm and (b) α between 440 and 870 nm for every site. The columns and bars represent the mean values the standard deviations, respectively.
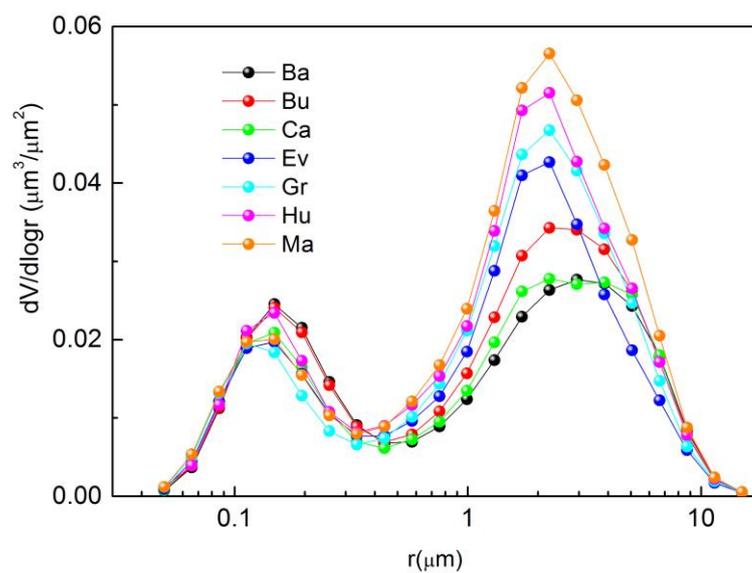
Figure 5. Annual mean particle size distribution for every site in 2010-2012.
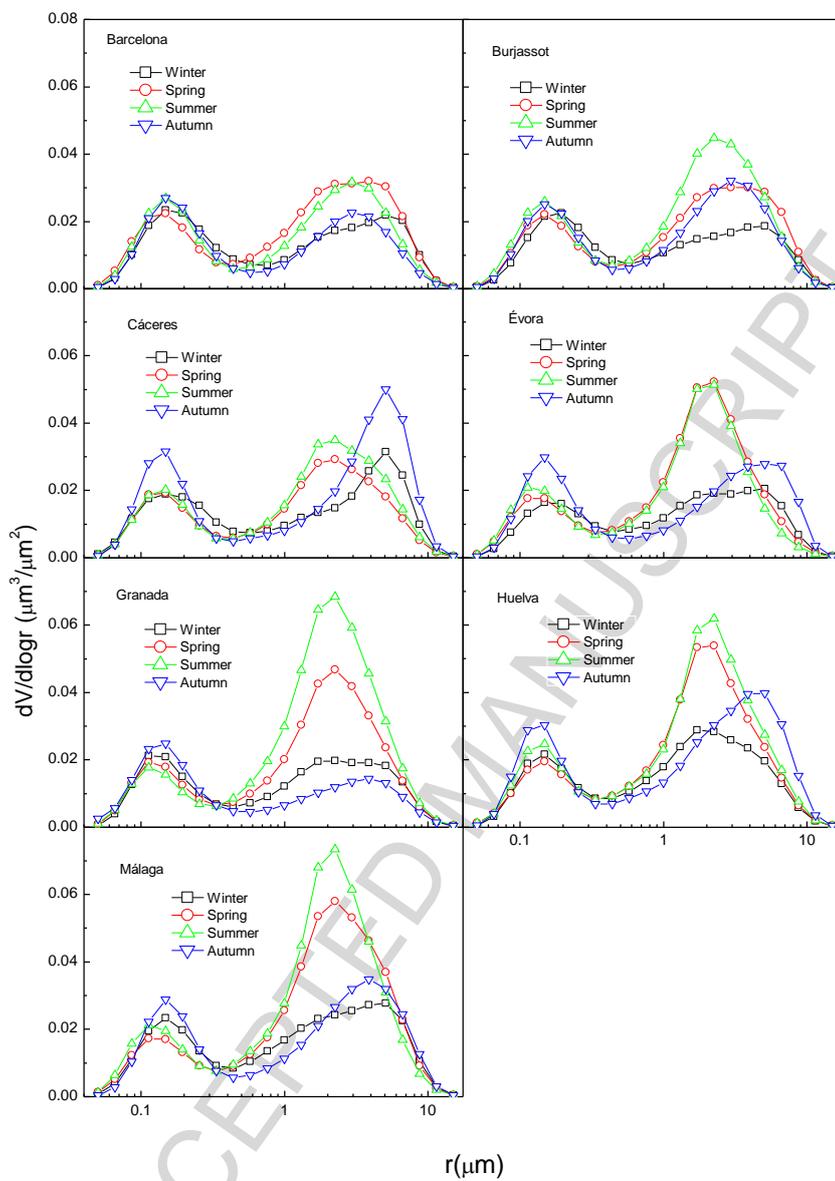
Figure 6. Seasonal mean particle size distribution for every site in 2010-2012.
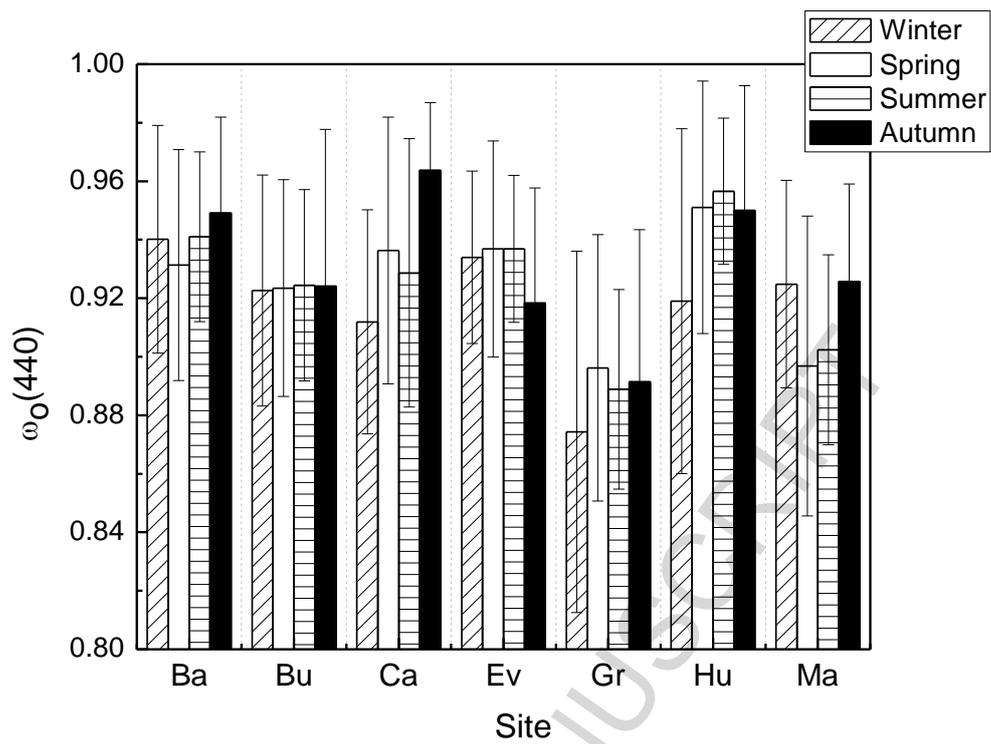
Figure 7. Seasonal dependence of ω_0 at 440 nm for every site. The columns and bars represent the mean values and the standard deviations, respectively.
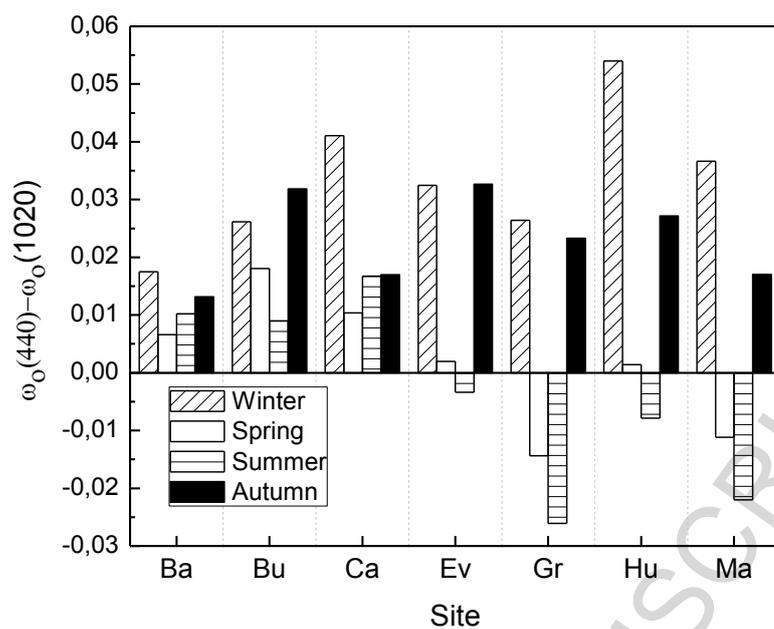
Figure 8. Seasonal dependence of $\Delta\omega_0$ [$\omega_0(440)$-$\omega_0(1020)$] for every site. The columns represent the mean values.
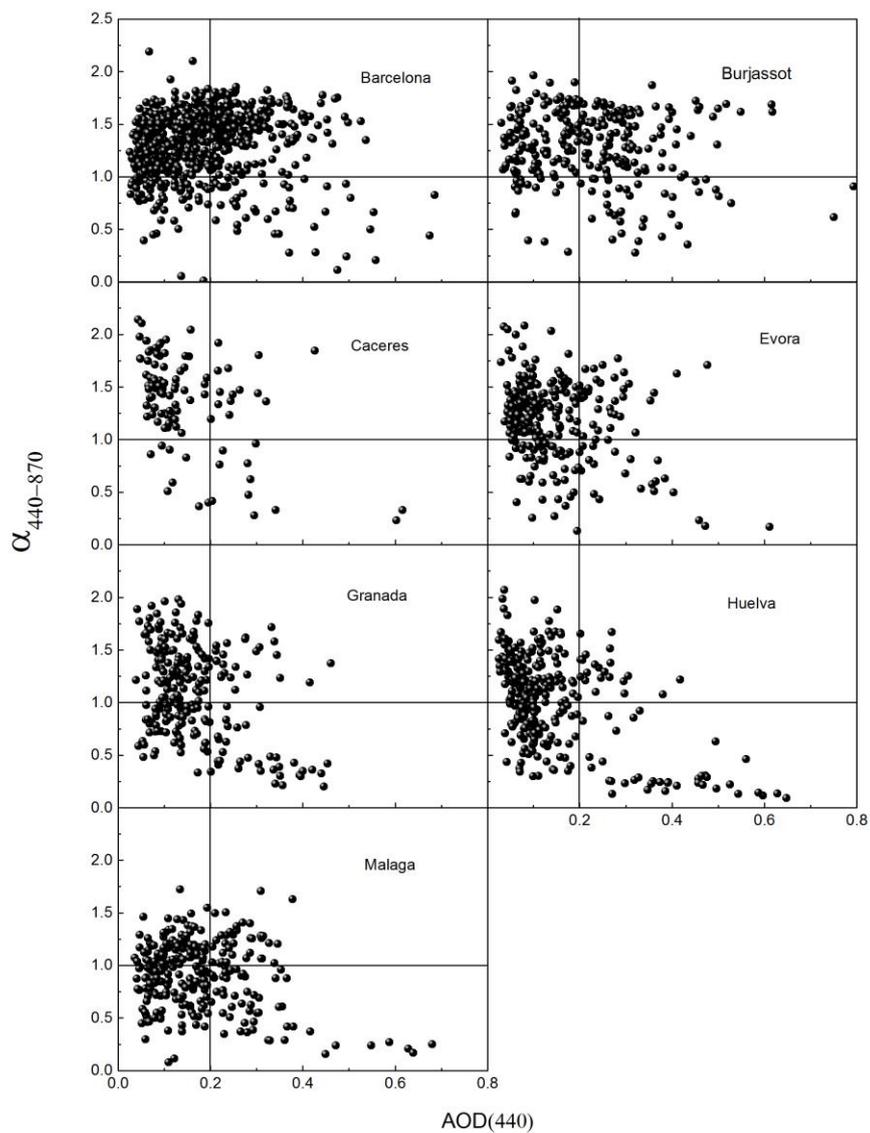
Figure 9. Scatter plots of α between 440 and 870 nm versus AOD at 440 nm for every site. Vertical and horizontal lines represent limit values for AOD and α, respectively.
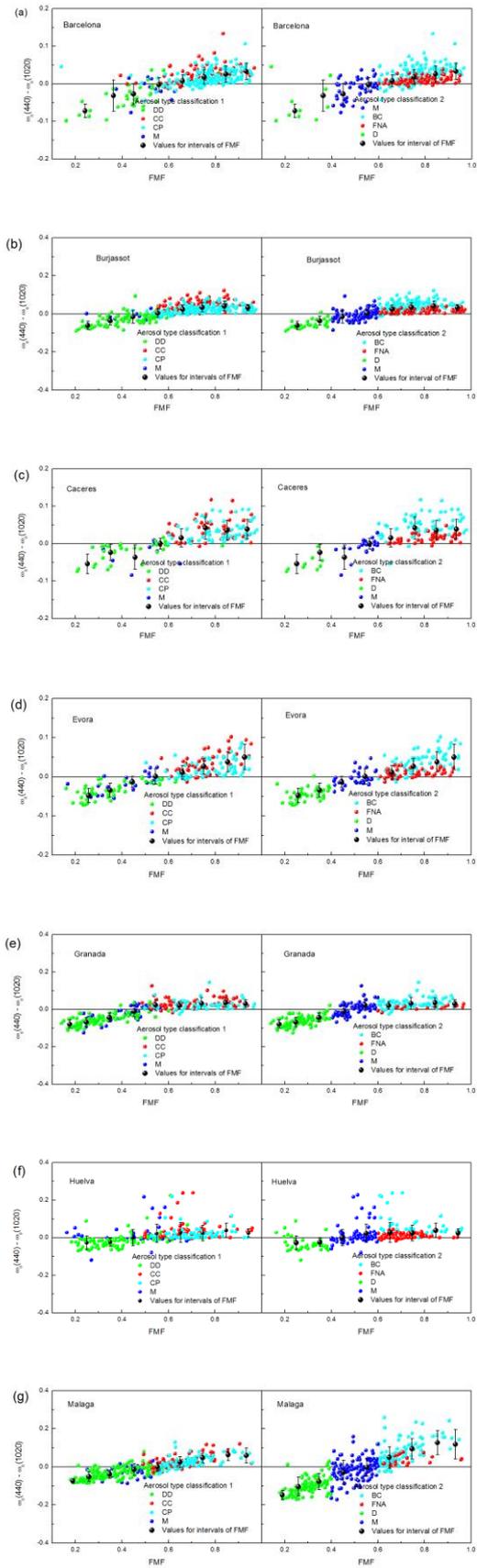
Figure 10. Relationship between $\Delta\omega_o$ [$(\omega_o(440)-\omega_o(1020))$] and FMF for every site considering both classifications: (a) Barcelona, (b) Burjassot, (c) Cáceres, (d) Évora, (e) Granada, (f) Huelva, (g) Málaga. Classification 1 refers to desert dust (DD), continental clean (CC), continental polluted (CP) and maritime (M). Classification 2 refers to absorbing fine mode (AF), non-absorbing fine mode (NAF), dust (D) and mixture (Mix).

Table 1: Statistical analysis from daily averages of AOD at 440 nm, α between 440 and 870 nm, and FMF for every site: number of data (N), standard deviation (SD), fifth percentile (P5) and ninety five percentile (P95).

	N	Mean±SD	P5	Median	P95
Barcelona					
AOD (440)	695	0.19±0.12	0.05	0.17	0.40
$\alpha_{440-870}$	695	1.31±0.32	0.72	1.37	1.74
FMF	562	0.68±0.14	0.43	0.68	0.89
Burjassot					
AOD (440)	918	0.18±0.13	0.04	0.16	0.43
$\alpha_{440-870}$	918	1.18±0.35	0.53	1.21	1.67
FMF	736	0.65±0.16	0.36	0.66	0.89
Cáceres					
AOD (440)	580	0.14±0.09	0.05	0.11	0.30
$\alpha_{440-870}$	580	1.28±0.38	0.54	1.31	1.82
FMF	466	0.72±0.17	0.37	0.75	0.95
Évora					
AOD (440)	771	0.13±0.10	0.04	0.10	0.33
$\alpha_{440-870}$	771	1.15±0.41	0.33	1.21	1.75
FMF	699	0.62±0.17	0.28	0.64	0.87
Granada					
AOD (440)	788	0.17±0.11	0.06	0.14	0.39
$\alpha_{440-870}$	788	1.00±0.44	0.25	0.99	1.69
FMF	643	0.55±0.19	0.24	0.53	0.87
Huelva					
AOD (440)	777	0.16±0.11	0.04	0.12	0.39
$\alpha_{440-870}$	777	0.93±0.41	0.21	0.98	1.52
FMF	690	0.58±0.19	0.25	0.60	0.88
Málaga					
AOD (440)	860	0.18±0.13	0.06	0.15	0.43
$\alpha_{440-870}$	860	0.93±0.35	0.32	0.96	1.48
FMF	775	0.53±0.16	0.27	0.53	0.78

Table 2: Median radius and standard deviation for fine and coarse mode by site and season.

Station	Radius (µm) Fine Mode	Radius (µm) Coarse Mode
Barcelona		
Winter	0.17±0.03	2.4±0.7
Spring	0.14±0.02	2.0±0.4
Summer	0.14±0.02	2.1±0.3
Autumn	0.16±0.02	2.3±0.4
Burjassot		
Winter	0.18±0.02	2.2±0.6
Spring	0.15±0.02	2.0±0.4
Summer	0.14±0.02	2.0±0.3
Autumn	0.18±0.02	2.2±0.2
Cáceres		
Winter	0.17±0.05	2.1±0.5
Spring	0.14±0.03	1.9±0.4
Summer	0.14±0.02	2.1±0.4
Autumn	0.14±0.02	2.4±0.5
Évora		
Winter	0.17±0.03	2.2±0.7
Spring	0.14±0.02	1.7±0.3
Summer	0.14±0.02	1.8±0.2
Autumn	0.15±0.02	2.3±0.5
Granada		
Winter	0.15±0.03	2.3±0.7
Spring	0.13±0.02	1.9±0.3
Summer	0.13±0.01	1.9±0.3
Autumn	0.14±0.02	2.3±0.5
Huelva		
Winter	0.15±0.02	1.9±0.6
Spring	0.15±0.02	1.8±0.3
Summer	0.14±0.02	1.9±0.3
Autumn	0.14±0.02	2.2±0.7
Málaga		
Winter	0.15±0.02	2.0±0.5
Spring	0.14±0.02	1.8±0.2
Summer	0.13±0.01	1.9±0.3
Autumn	0.15±0.02	2.1±0.3

Table 3: Statistical analysis from daily averages of ω_0 at 440, 675, 870 and 1020 nm for every site: number of data (N), standard deviation (SD), fifth percentile (P5) and ninety five percentile (P95).

	N	Mean±SD	P5	Median	P95
Barcelona					
ω_0 (440)	306	0.94 ± 0.04	0.87	0.94	0.99
ω_0 (675)	306	0.94 ± 0.04	0.87	0.94	0.99
ω_0 (870)	306	0.93 ± 0.04	0.85	0.93	0.99
ω_0 (1020)	306	0.93 ± 0.05	0.84	0.93	0.99
Burjassot					
ω_0 (440)	401	0.92 ± 0.04	0.86	0.92	0.99
ω_0 (675)	401	0.91 ± 0.05	0.83	0.92	0.99
ω_0 (870)	401	0.91 ± 0.05	0.81	0.92	0.98
ω_0 (1020)	401	0.91 ± 0.06	0.81	0.92	0.98
Cáceres					
ω_0 (440)	150	0.93 ± 0.05	0.85	0.94	0.99
ω_0 (675)	150	0.92± 0.05	0.83	0.94	0.99
ω_0 (870)	150	0.92 ± 0.6	0.80	0.93	0.99
ω_0 (1020)	150	0.91 ± 0.06	0.79	0.93	0.99
Évora					
ω_0 (440)	185	0.94 ± 0.03	0.89	0.93	0.99
ω_0 (675)	185	0.93 ± 0.04	0.86	0.94	0.99
ω_0 (870)	185	0.93 ± 0.05	0.84	0.94	0.99
ω_0 (1020)	185	0.93 ± 0.05	0.83	0.94	0.99
Granada					
ω_0 (440)	269	0.89 ± 0.05	0.82	0.89	0.96
ω_0 (675)	269	0.90 ± 0.05	0.81	0.91	0.96
ω_0 (870)	269	0.90 ± 0.06	0.78	0.91	0.97
ω_0 (1020)	269	0.90 ± 0.07	0.76	0.91	0.97
Huelva					
ω_0 (440)	270	0.95 ± 0.04	0.85	0.95	0.99
ω_0 (675)	270	0.94 ± 0.06	0.80	0.96	0.99
ω_0 (870)	270	0.94 ± 0.07	0.77	0.96	0.99
ω_0 (1020)	270	0.94 ± 0.07	0.76	0.96	0.99
Málaga					
ω_0 (440)	332	0.91 ± 0.04	0.83	0.91	0.97
ω_0 (675)	332	0.91 ± 0.05	0.82	0.91	0.97
ω_0 (870)	332	0.91 ± 0.05	0.82	0.92	0.98
ω_0 (1020)	332	0.91 ± 0.05	0.82	0.92	0.98

Table 4. Relative frequency, mean and standard deviation (SD) of AOD at 440 nm and α between 440 and 870 nm for each aerosol type based on the AOD(440) and $\alpha_{440-870}$ classification (classification 1) for every site. The different aerosol types are maritime (M), continental clean (CC), continental polluted (CP) and desert dust (DD).

Site	Aerosol Type	Relative Frequency (%)	AOD(440) Mean±SD	$\alpha_{440-870}$ Mean±SD
Barcelona	M	8.6	0.10±0.05	0.80±0.20
	CC	50.8	0.12±0.05	1.38±0.21
	CP	33.5	0.28±0.07	1.47±0.20
	DD	7.1	0.38±0.20	0.69±0.23
Burjassot	M	16.3	0.08±0.04	0.78±0.18
	CC	45.3	0.11±0.05	1.33±0.21
	CP	26.6	0.30±0.08	1.38±0.21
	DD	11.8	0.37±0.14	0.67±0.24
Cáceres	M	15.9	0.11±0.04	0.79±0.19
	CC	64.3	0.10±0.04	1.43±0.25
	CP	13.1	0.28±0.09	1.45±0.22
	DD	6.7	0.31±0.10	0.62±0.25
Évora	M	20.9	0.11±0.04	0.68±0.24
	CC	61.2	0.09±0.04	1.35±0.23
	CP	9.7	0.26±0.06	1.43±0.21
	DD	8.2	0.34±0.14	0.52±0.28
Granada	M	32.4	0.12±0.04	0.74±0.19
	CC	42.1	0.12±0.04	1.37±0.23
	CP	7.6	0.26±0.05	1.38±0.20
	DD	17.9	0.33±0.12	0.45±0.24
Huelva	M	37.2	0.10±0-04	0.66±0.26
	CC	37.7	0.11±0.04	1.28±0.20
	CP	10.0	0.28±0.10	1.30±0.17
	DD	15.1	0.34±0.11	0.49±0.29
Málaga	M	33.2	0.11±0.04	0.74±0.18
	CC	34.7	0.11±0.04	1.23±0.16
	CP	11.0	0.28±0.06	1.29±0.18
	DD	21.2	0.35±0.14	0.54±0.24

Table 5. Relative frequency, mean and standard deviation (SD) of AOD at 440 nm and α between 440 and 870 nm for each aerosol type based on the FMF and ω_o at 440 nm classification (classification 2) for every site. The different aerosol types are absorbing fine mode (AF), non-absorbing fine mode (NAF), dust (D) and mixture (Mix).

Site	Aerosol Type	Relative Frequency (%)	AOD(440) Mean±SD	$\alpha_{440-870}$ Mean±SD
Barcelona	NAF	28.6	0.26±0.09	1.51±0.18
	AF	49.8	0.24±0.08	1.48±0.21
	D	3.2	0.39±0.16	0.51±0.50
	Mix	17.1	0.27±0.13	0.86±0.26
Burjassot	NAF	19.5	0.32±0.11	1.43±0.20
	AF	47.2	0.23±0.07	1.43±0.19
	D	7.9	0.40±0.14	0.39±0.15
	Mix	23.7	0.27±0.09	0.92±0.19
Cáceres	NAF	30.7	0.22±0.06	1.43±0.24
	AF	40.5	0.23±0.10	1.50±0.22
	D	7.2	0.32±0.14	0.39±0.14
	Mix	15.0	0.24±0.06	0.91±0.23
Évora	NAF	23.3	0.23±0.06	1.32±0.30
	AF	36.5	0.21±0.06	1.45±0.20
	D	19.6	0.32±0.14	0.33±0.15
	Mix	17.5	0.23±0.07	0.80±0.14
Granada	NAF	6.0	0.26±0.09	1.47±0.27
	AF	29.4	0.21±0.05	1.39±0.17
	D	34.4	0.30±0.13	0.35±0.15
	Mix	29.8	0.20±0.04	0.90±0.20
Huelva	NAF	30.2	0.23±0.07	1.26±0.25
	AF	16.0	0.22±0.08	1.28±0.28
	D	14.2	0.34±0.16	0.26±0.15
	Mix	28.0	0.23±0.08	0.81±0.27
Málaga	NAF	5.4	0.29±0.11	1.36±0.19
	AF	25.4	0.22±0.06	1.34±0.18
	D	28.9	0.36±0.16	0.39±0.15
	Mix	37.1	0.23±0.08	0.88±0.18

Table 6. Relative frequency of fine (FMF > 0.6), coarse (FMF < 0.4) and mixture (0.4 < FMF < 0.6). Parenthesis refers to the fraction of absorbing aerosol in each sub-type.

Fine (Absorbing) (%)	Mixture (Absorbing) (%)	Coarse (Absorbing) (%)
Barcelona		
79	17	4
(63)	(62)	(83)
Burjassot		
67	24	9
(71)	(82)	(82)
Cáceres		
72	15	13
(68)	(61)	(47)
Évora		
60	18	22
60	(61)	(85)
Granada		
38	28	35
(83)	(96)	(99)
Huelva		
46	28	26
(34)	(47)	(54)
Málaga		
32	35	33
(82)	(83)	(90)

Table 7. Relative frequency for each aerosol type based on the FMF and ω_o at 440 nm classification (classification 2) for every site. The different aerosol types are absorbing fine mode (AF), non-absorbing fine mode (NAF), dust (D) and mixture (Mix).

	AF	NAF	D	Mix
Barcelona	**50.0**	**28.2**	**3.2**	**17.3**
Winter	49.3	28.4	1.5	20.9
Spring	48.9	21.6	8.0	21.6
Summer	53.8	30.8	0.9	14.5
Autumn	41.4	45.5	3.0	9.1
Burjassot	**48.0**	**20.1**	**7.8**	**24.1**
Winter	54.4	28.1	7.0	10.5
Spring	52.0	18.1	7.9	20.0
Summer	44.4	14.6	8.8	32.2
Autumn	48.5	33.3	0	18.2
Cáceres	**43.6**	**33.6**	**6.4**	**16.4**
Winter	77.8	11.1	7.4	3.7
Spring	41.3	28.3	2.2	28.3
Summer	35.2	43.5	11.1	16.7
Autumn	15.4	84.6	0	0
Évora	**37.4**	**24.6**	**19.6**	**18.4**
Winter	53.6	28.6	7.1	10.7
Spring	21.9	28.1	25.0	25.0
Summer	38.9	20.8	20.8	19.5
Autumn	66.7	20.0	13.3	0.0
Granada	**30.7**	**6.0**	**35.2**	**28.1**
Winter	63.6	15.9	4.6	15.9
Spring	26.8	7.0	35.2	31
Summer	13.4	1.5	52.0	33.1
Autumn	72.0	8.0	4.0	16
Huelva	**17.9**	**34.6**	**15.4**	**32.1**
Winter	29.8	25.5	19.2	25.5
Spring	15.0	37.5	15.0	32.5
Summer	12.5	36.3	17.5	33.7
Autumn	21.2	36.4	6.0	36.4
Málaga	**26.7**	**5.9**	**30.4**	**37.0**
Winter	54.5	15.9	9.1	20.5
Spring	27.5	3.7	29.4	39.4
Summer	13.6	2.1	42.1	42.1

Table 8. Fitting parameters of $\Delta\omega_o$ [$\omega_o(440)$-$\omega_o(1020)$] versus FMF for every site.

a	b	c	R^2
Barcelona			
-0.14±0.008	0.34±0.03	-0.16±0.03	0.99
Burjassot			
-0.16±0.01	0.44±0.04	-0.25±0.03	0.99
Cáceres			
-0.11±0.03	0.24±0.10	-0.09±0.08	0.90
Évora			
-0.10±0.01	0.21±0.04	-0.06±0.03	0.99
Granada			
-0.16±0.01	0.44±0.05	-0.25±0.05	0.97
Huelva			
-0.11±0.02	0.34±0.09	-0.20±0.07	0.91
Málaga			
-0.12±0.01	0.26±0.04	-0.06±0.04	0.99

Table 9. Fitting parameters of $\Delta\omega_o/\omega_o(440)$ versus FMF for every site.

a	b	c	R^2
Barcelona			
-0.13±0.02	0.29±0.07	-0.12±0.0	0.98
Burjassot			
-0.19±0.02	0.53±0.08	-0.30±0.06	0.97
Cáceres			
-0.13±0.04	0.28±0.16	-0.10±0.13	0.86
Évora			
-0.10±0.01	0.21±0.03	-0.04±0.03	0.99
Granada			
-0.19±0.02	0.54±0.08	-0.32±0.07	0.96
Huelva			
-0.11±0.02	0.37±0.08	-0.23±0.07	0.91
Málaga			
-0.14±0.02	0.33±0.06	-0.11±0.05	0.98

Highlights:

- Derivation of $\Delta\omega o$ under scenarios of no sky radiance measurements

- Relationship $\Delta\omega o/\omega o$ and FMF is an appropriate tool for aerosol typying